Master in Electrical and Electronics Engineering

EE-517: Bio-Nano-Chip Design

Lecture #9

Nanotechnology to enhance Electron Transfer

Lecture Outline

(Book Bio/CMOS: Chapter' paragraphs §8.9.1-4)

- Electrochemistry of CNT
- Nernst effect with CNT
- Layering effect with CNT
- Cottrell effect with CNT
- Randle-Sevčhik effect with CNT
- Electron Transfer with CNT
- Electrons emission from tips and lateral side-walls

CMOS/Sample interface

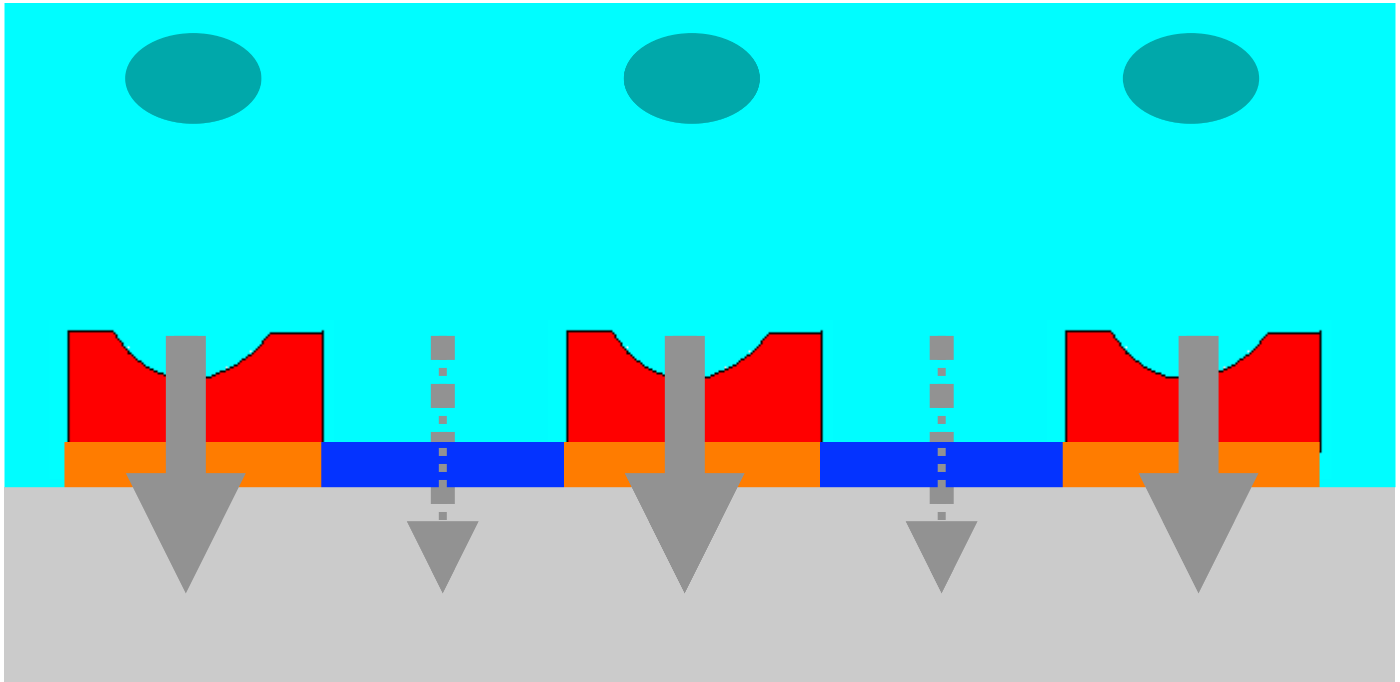

The interface between the CMOS circuit and the bio-sample needs to be deeply investigated and organized

Carbon Nanotubes

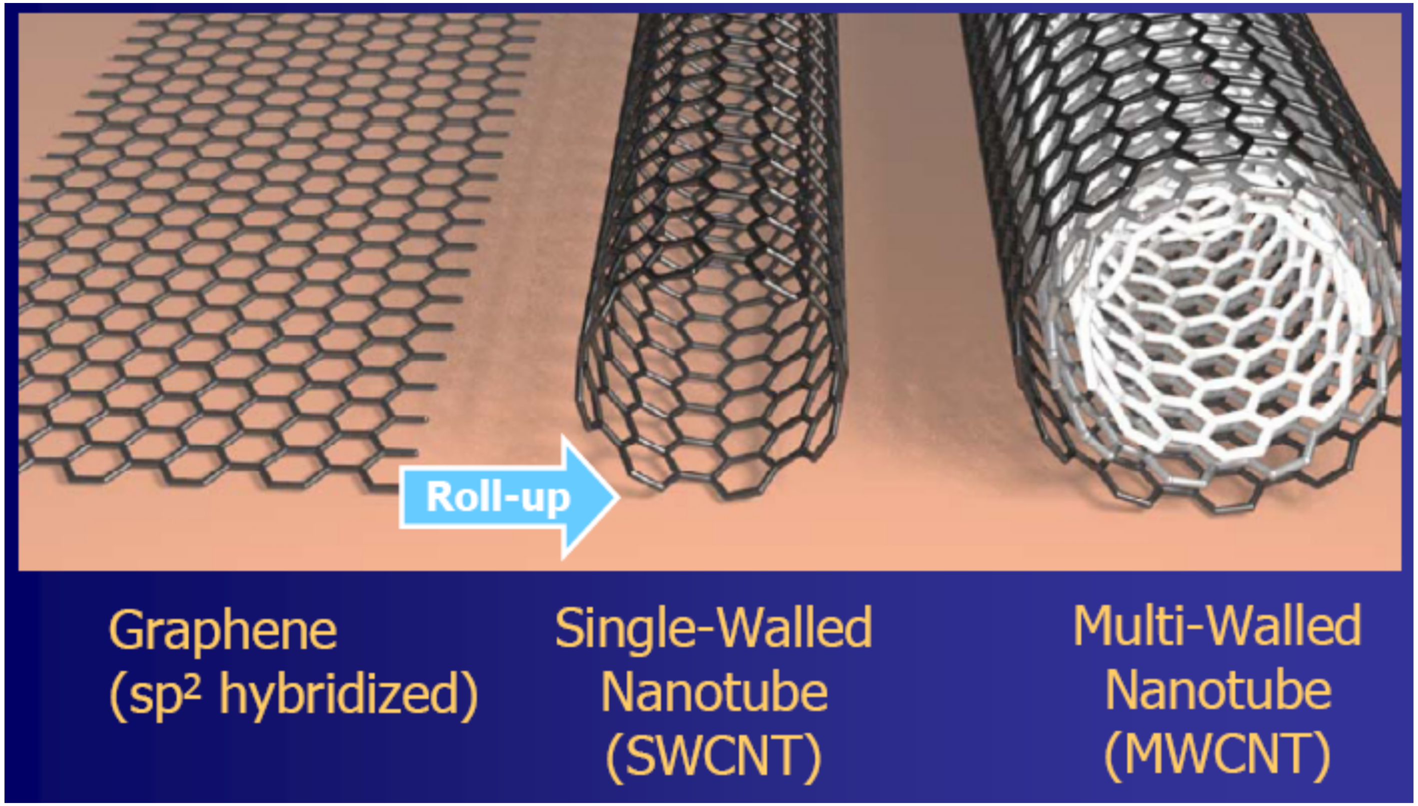

Courtesy: K. Banerjee/California Univ.

CNT electrical conductivity

	Cu	SWCNT	MWCNT
Max current density (A/cm^2)	$<1x10^7$	$>1x10^9$ Radosavljevic, et al., *Phys. Rev. B*, 2001	
Thermal conductivity (W/mK)	385	5800 Hone, et al., *Phys. Rev. B*, 1999	3000 Kim, et al., *Phys. Rev. Let.*, 2001
Mean free path (nm) @ room temp	40	>1,000 McEuen, et al., *Trans. Nano.*, 2002	25,000 Li, et al., *Phys. Rev. Let.*, 2005

Single Walled or Multi-Walled Carbon Nanotubes leads to different electrical properties

CMOS/CNT/Bio Interface

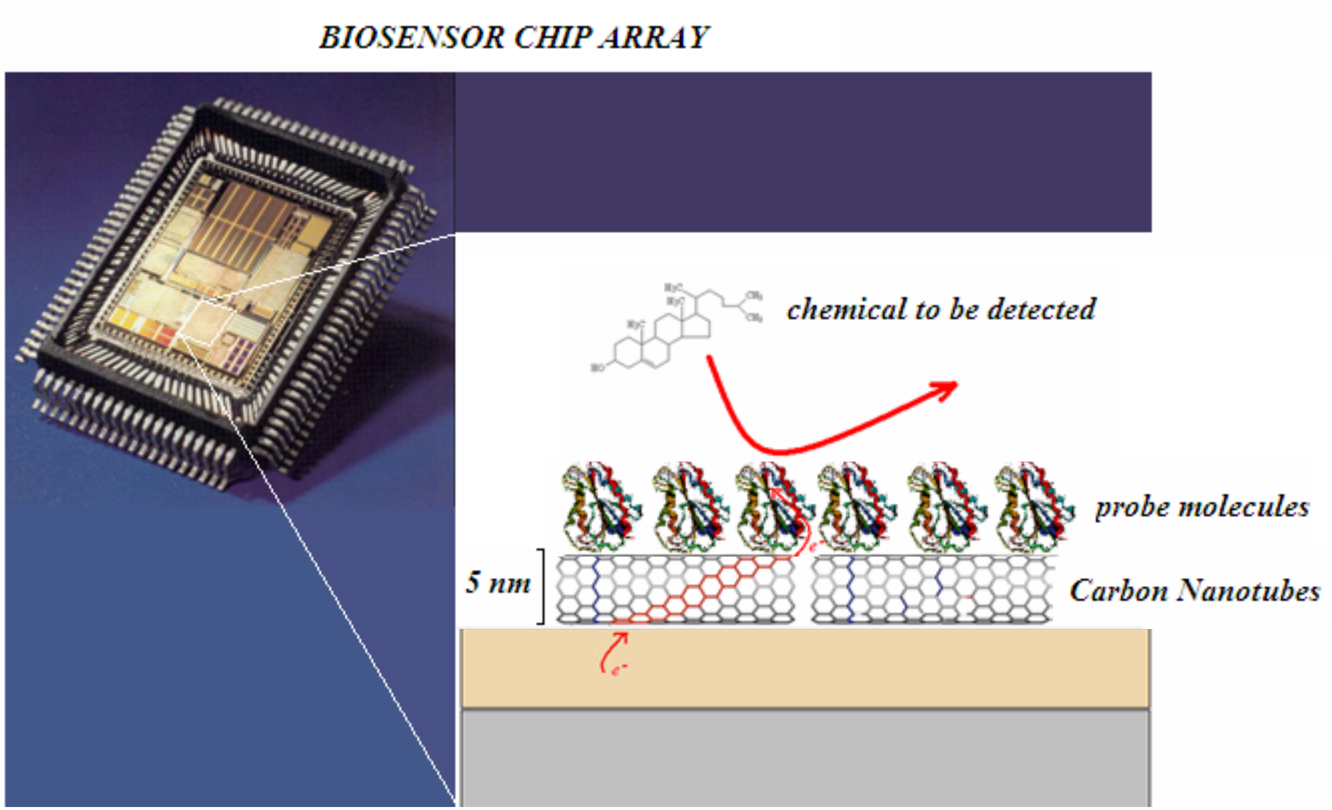

Carbon Nanotubes improve the Electron Transfer from chemicals to sensing electrode

Methods for CNT deposition

- Drop casting
- Micro-spotting
- Electrodeposition
- Growth by Chemical Vapour Deposition

Nano-Bio-Sensors integration

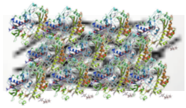

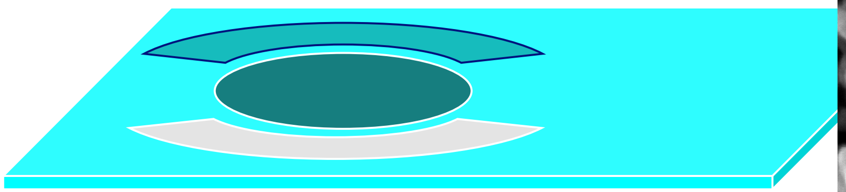

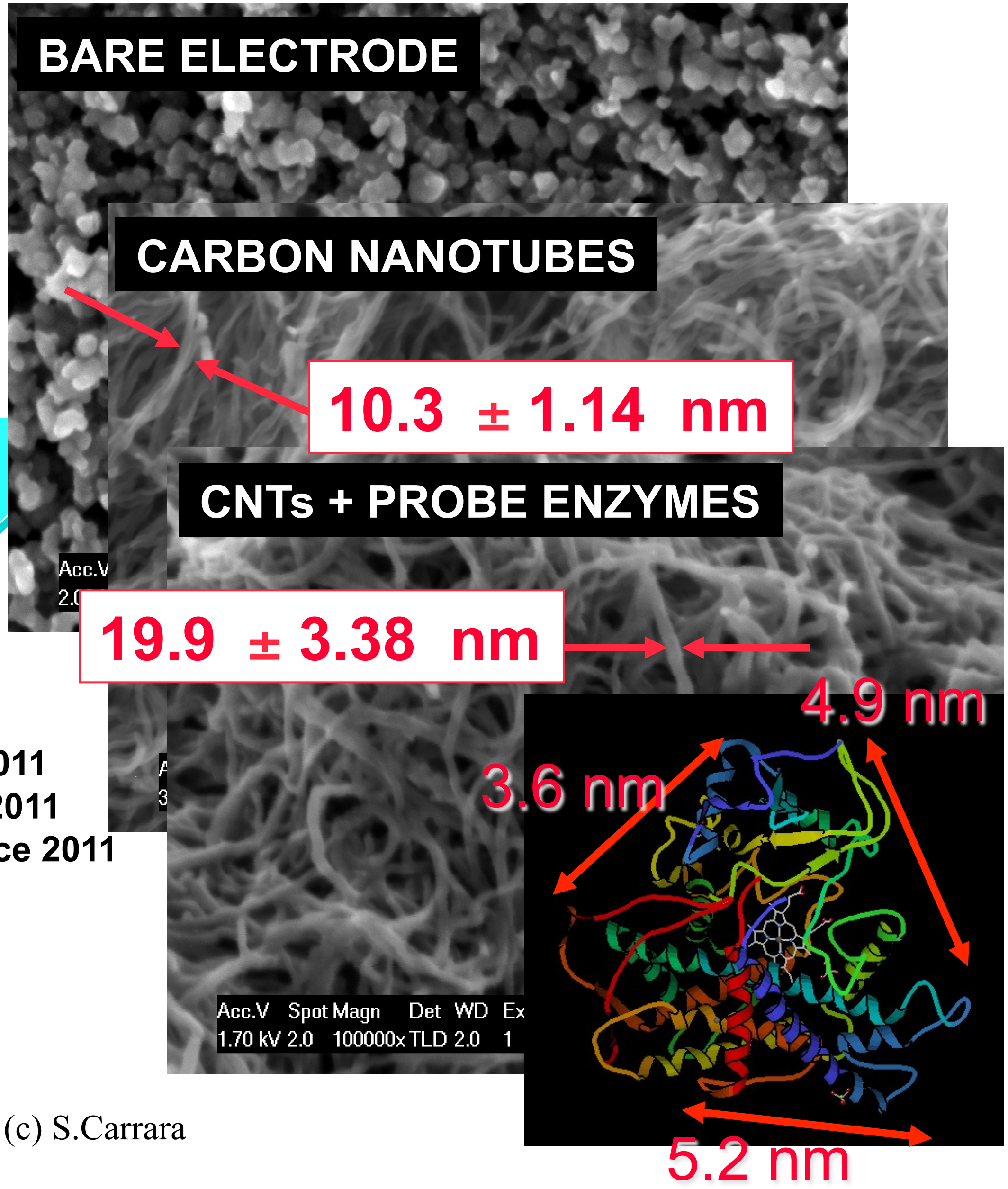

Boero, Carrara et al. / IEEE PRIME 2009
Boero, Carrara et al. / IEEE ICME 2010
De Venuto, al. et Carrara / IEEE Senors 2010
Boero, Carrara et al. / Sensors & Actuators B 2011
Carrara et al. / Biosensors and Bioelectronics 2011
Boero, Carrara et al. / IEEE T on NanoBioScience 2011

Nano-Bio-Sensors Micro-Spotting

Boero, Carrara et al. / IEEE BioCAS 2011

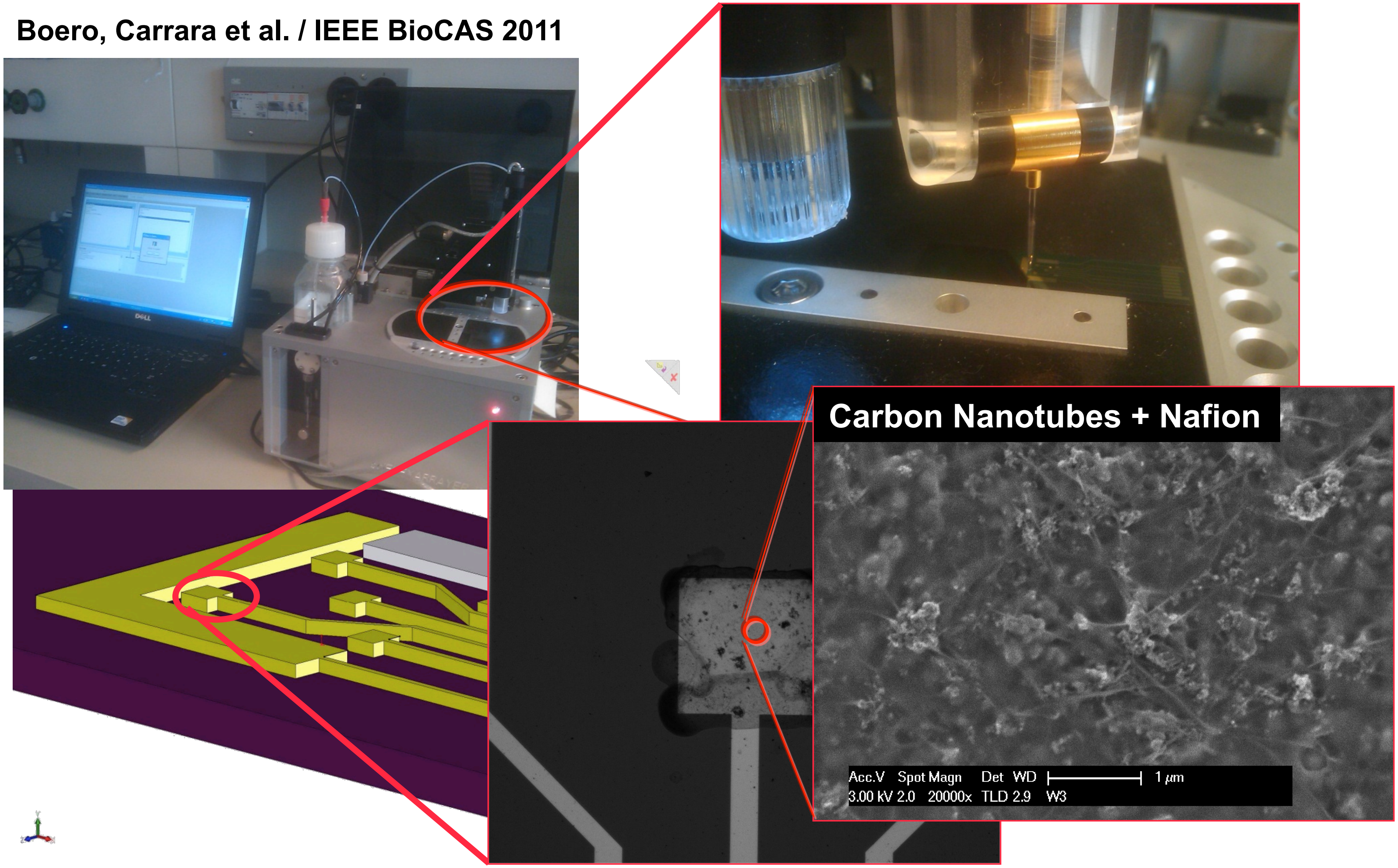

Nano-Bio-Sensors by Electrodeposition

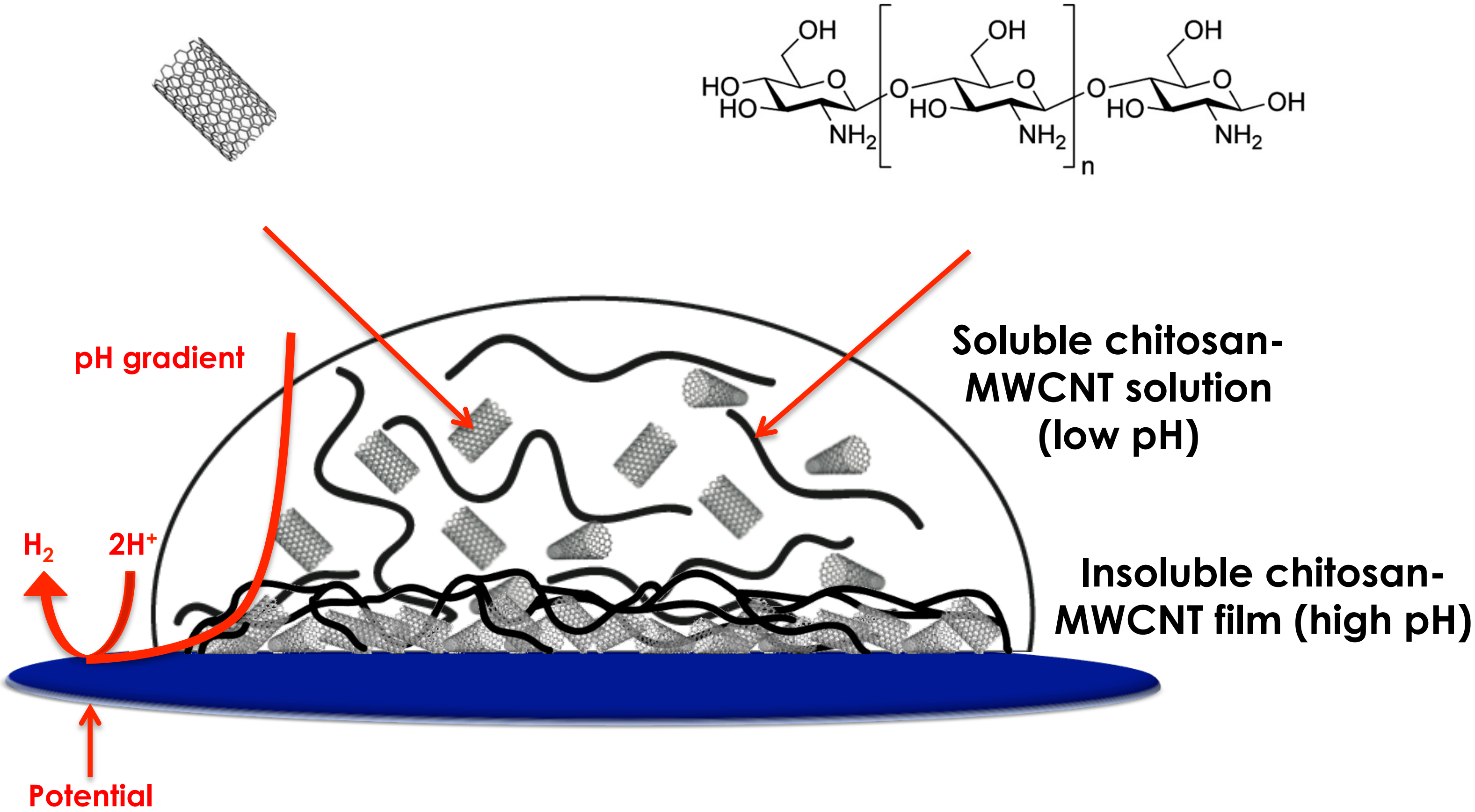

Nano-Bio-Sensors by Electrodeposition

DROP-CASTING

Results

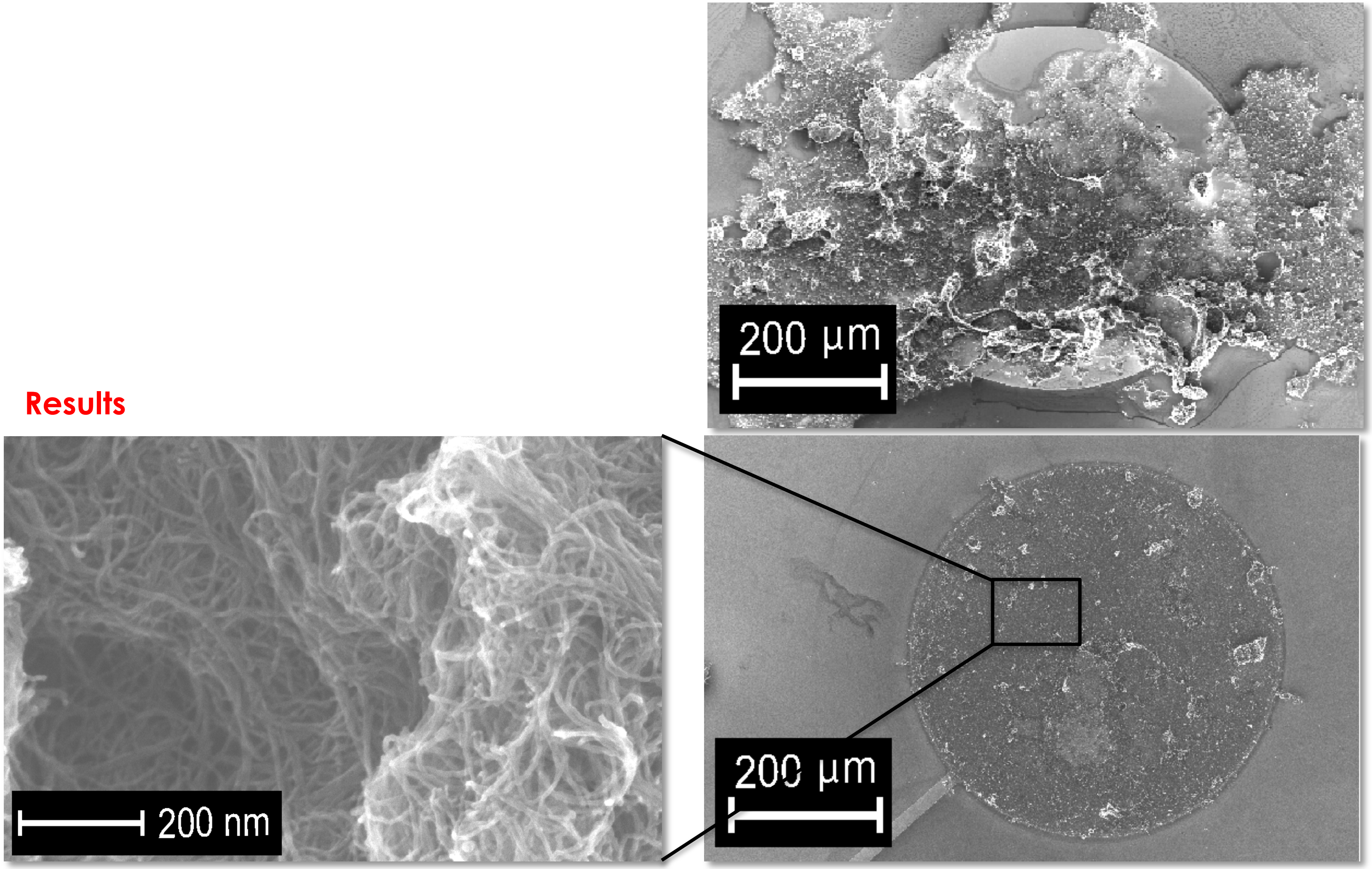

(c) S.Carrara

ELECTRODEPOSITION

Nano-Bio-Sensors by CVD

Integration by Direct Growth

Step I Catalyst electrodeposition

Step II Annealing (3-10 minutes)

Step III Deposition (CO_2 and C_2H_2 flow)

Taurino, Carrara et al. / UE Patent 2013

Down now till 450 °C
To be fully CMOS-compatible

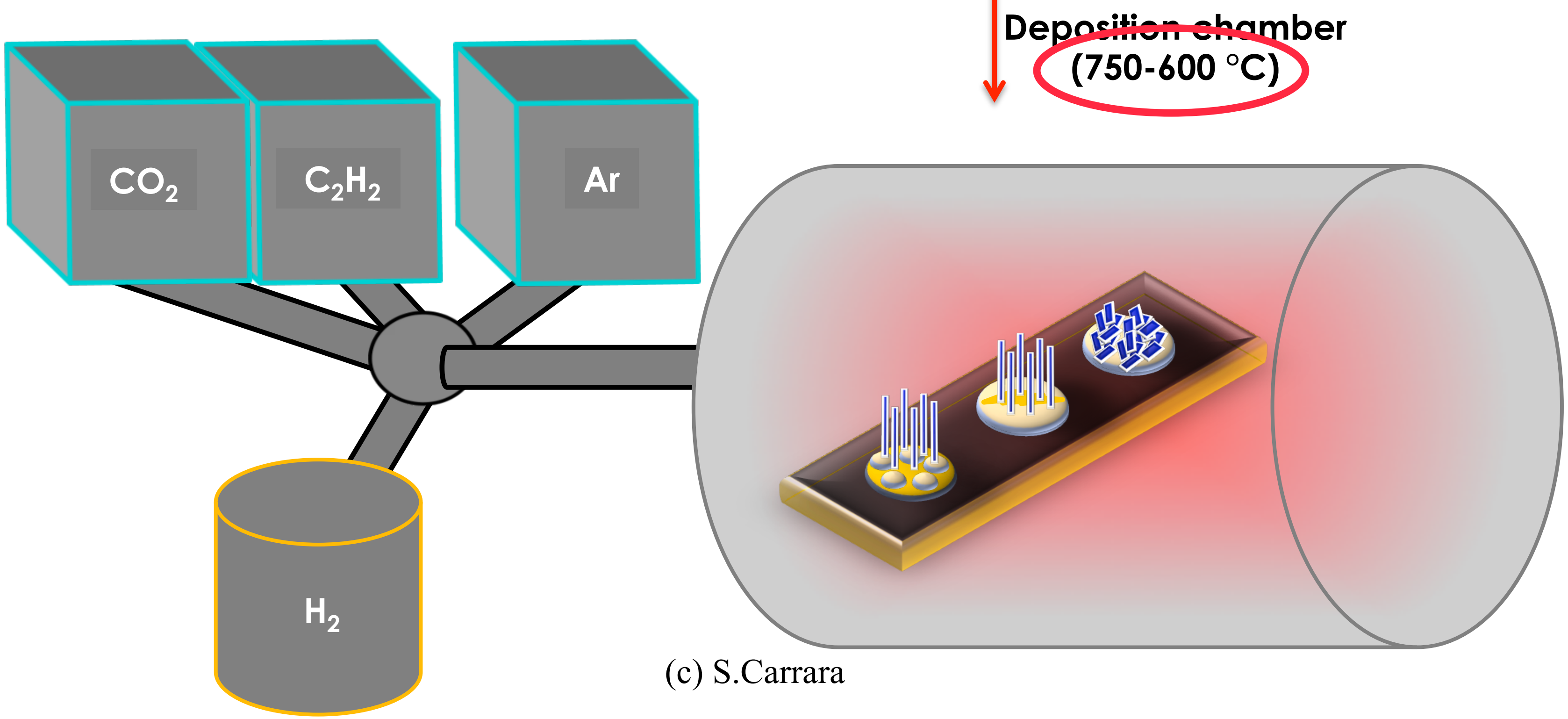

(c) S.Carrara

Nano-Bio-Sensors by CVD

Results

1. **Fe electrodeposition**
2. **Deposition**
   - *10 min annealing*
   - *5 min deposition*
   - *750 °C*
   - *0.25 l/h C_2H_2 flow*
   - *0.25 l/h CO_2 flow*

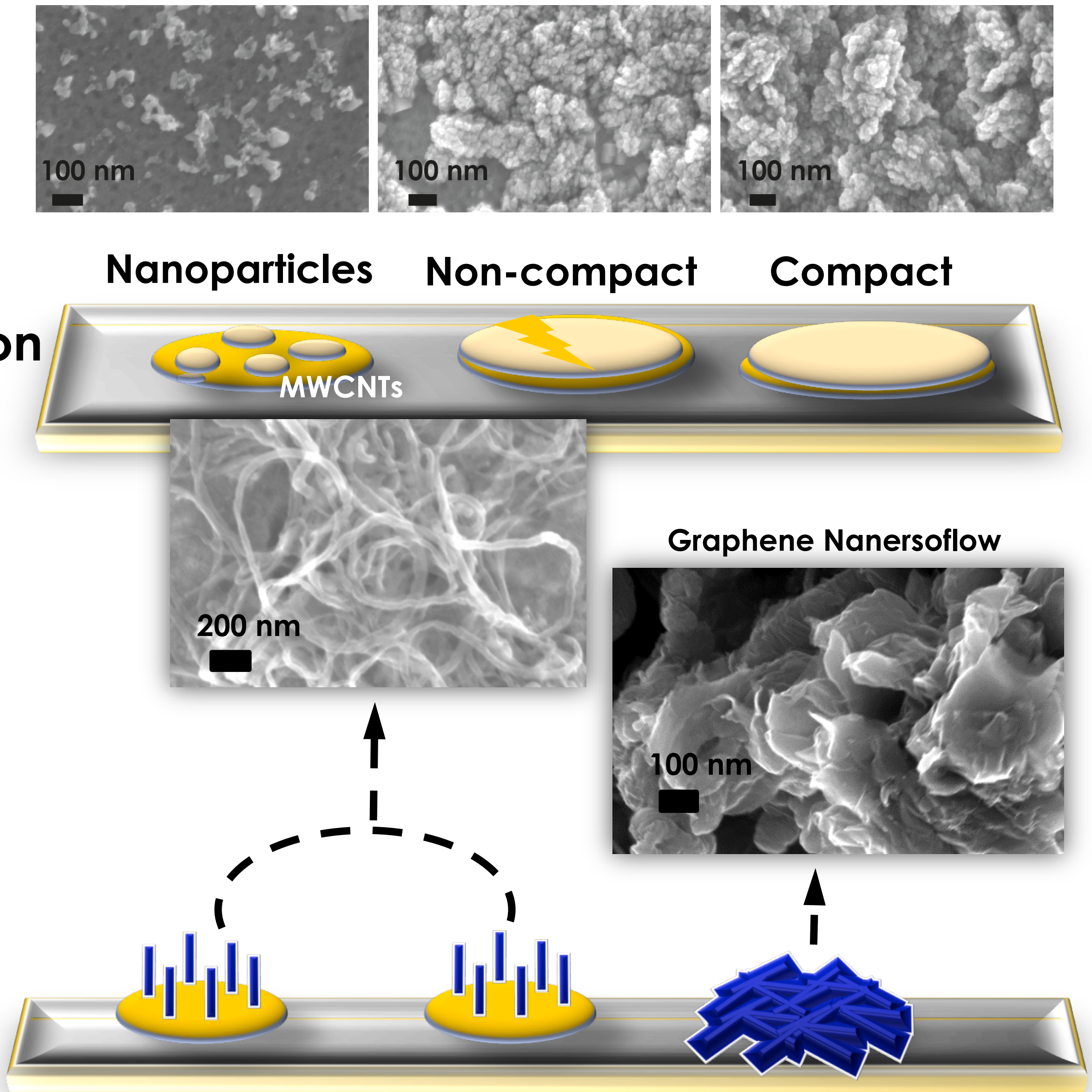

Carbon Nanotubes contribute to Redox Reactions Efficiency

Nernst equation

$$E = E^0 - \frac{RT}{nF} \ln\left(\frac{C_R(0,t)}{C_O(0,t)}\right)$$

Randles-Sevčik equation

$$i(0,t) \propto nFAD\left(\frac{nF\nu D}{RT}\right)^{1/2} C(0,t)$$

Cottrell equation

$$i(x,t) = \frac{nFAD^{1/2}C(x,t)}{\pi^{1/2}t^{1/2}}$$

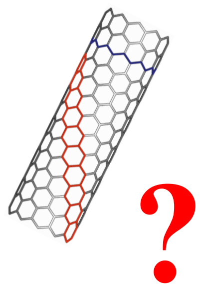

Geometrical Area vs Active Area

$$i(x,t) = \frac{nFA\sqrt{D}C(x,t)}{\sqrt{\pi t}}$$

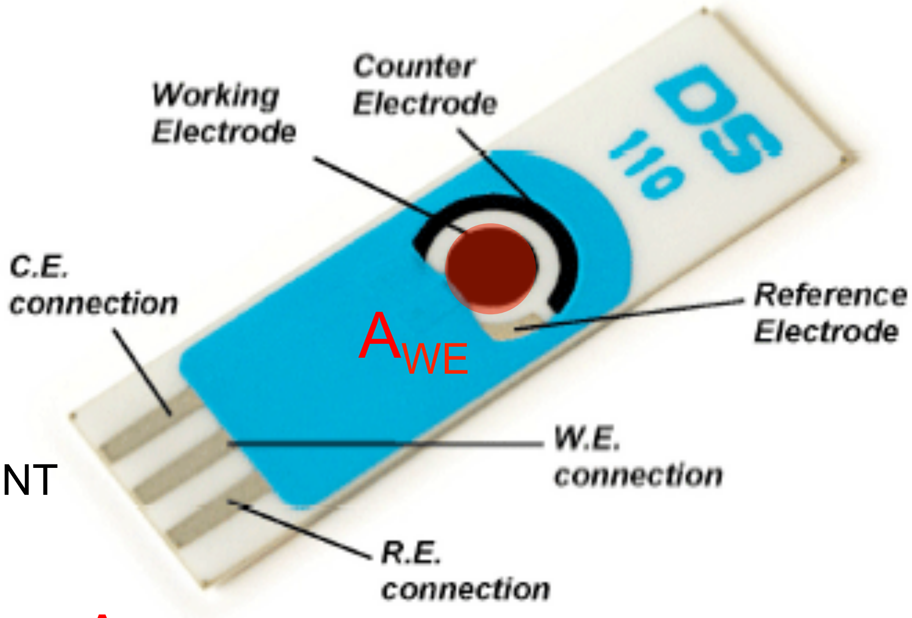

$A_{active}=A_{WE}+A_{CNT}$

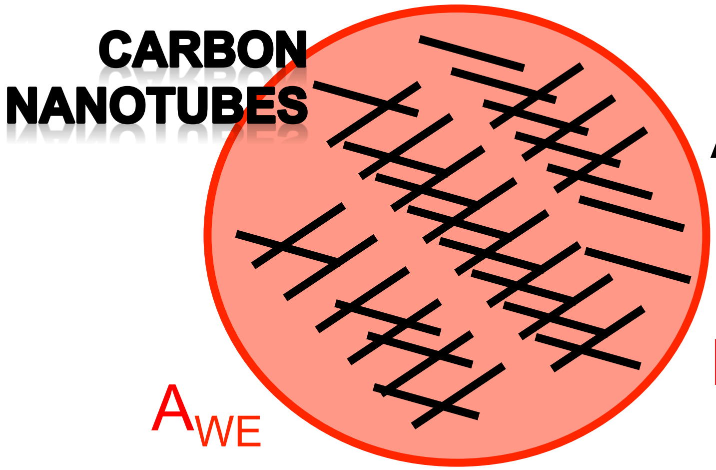

$A_{active}>A_{WE}$

$$i(x,t) = \frac{nFA_{Active}\sqrt{D}C(x,t)}{\sqrt{\pi t}}$$

Electrochemically Active Area

Sensitivity per unit area

- Sensitivity: metric considerations

$$S = \frac{\Delta i}{\Delta C} = \frac{1\,\mu A}{40\,\mu M} = 25\,\frac{mA}{M}$$

Total sensitivity without taking into account the different geometries of working electrodes in different sensors

$$S_A = \frac{\Delta i}{\Delta C \cdot A_{WE}} = \frac{1\,\mu A}{40\,\mu M \cdot 0.2 cm^2} = 125\,\frac{nA}{\mu M \cdot cm^2}$$

Sensitivity per unit-of-area, which normalizes for the geometries of working electrodes in different sensors

Geometrical Area vs Active Area

$$i(x,t) = \frac{nFA\sqrt{D}C(x,t)}{\sqrt{\pi t}}$$

?

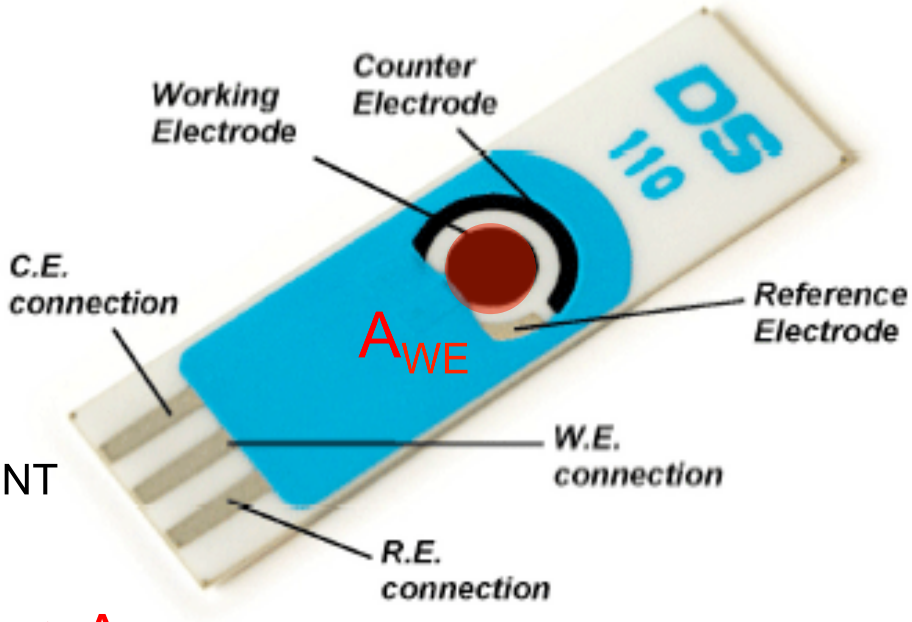

$A_{active}=A_{WE}+A_{CNT}$

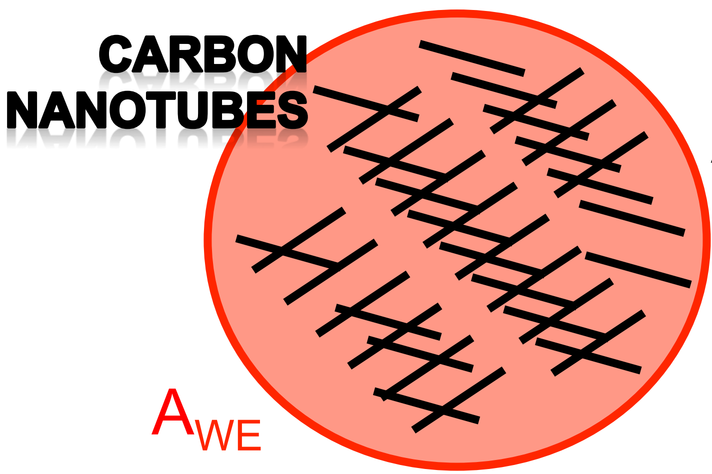

$A_{active}>A_{WE}$

Electrochemically Active Area

$$j = \frac{i}{A_{WE}} = \frac{nFA_{Active}\sqrt{DC}}{A_{WE}\sqrt{\pi t}}$$

Sensitivity per unit area

- Sensitivity as increased by CNT

$$S_A = \frac{\Delta i}{\Delta C \cdot A_{WE}} = \frac{nFA_{Active}\sqrt{D}}{A_{WE}\sqrt{\pi t}} = \frac{nF(A_{WE} + A_{CNT})\sqrt{D}}{A_{WE}\sqrt{\pi t}}$$

Active area increases due to CNT

Redox with oxidases

The hydrogen peroxide provides two possible redox reactions.
An oxidation:

$$H_2O_2 \xrightarrow{+650\ mV} O_2 + 2H^+ + 2e^-$$

And a reduction (of the oxygen):

$$O_2 + 4H^+ + 4\ e^- \xrightarrow{-700\ mV} 2H_2O$$

Redox with hydrogen peroxide

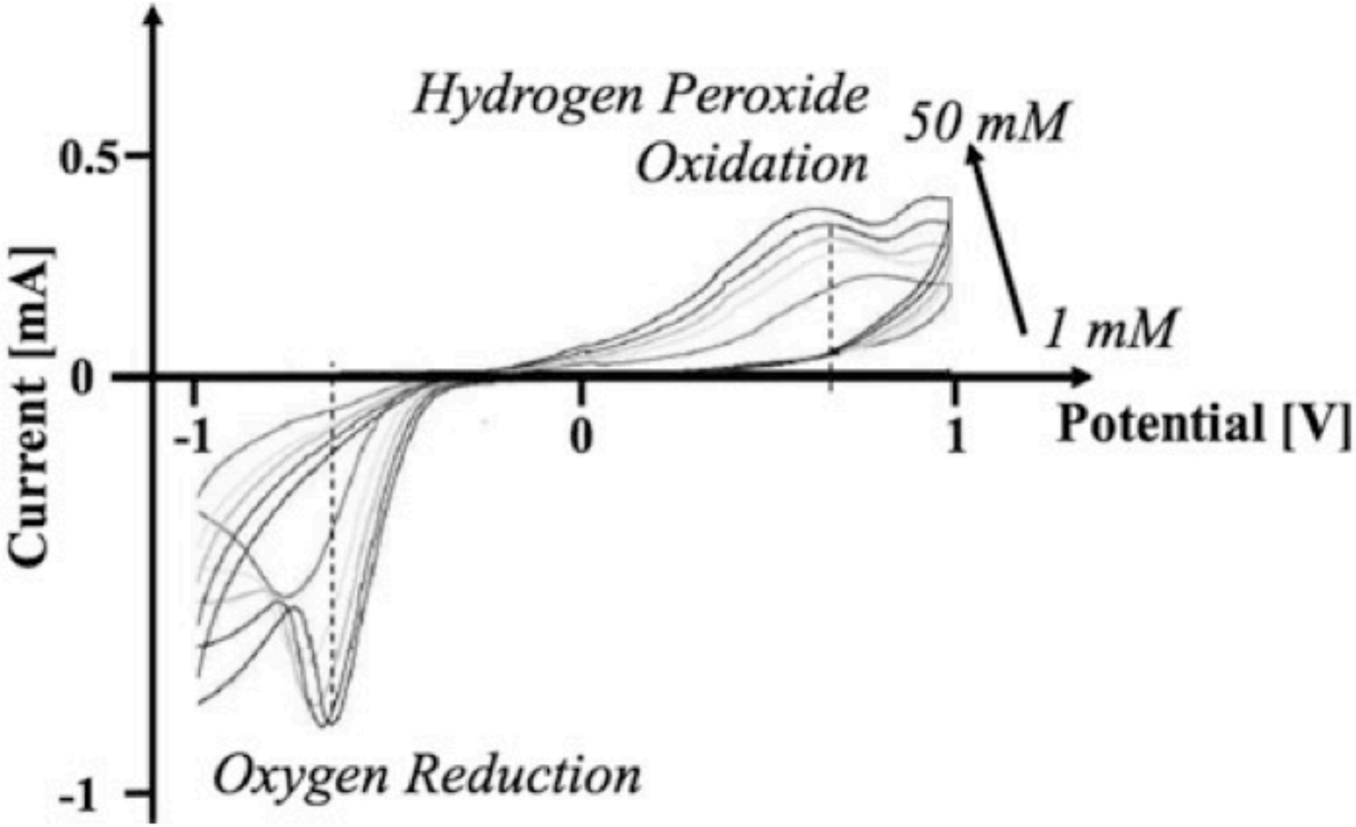

O_2 reduction and H_2O_2 oxidation observed by potential sweeping

Nernst Effect on H_2O_2 oxidation

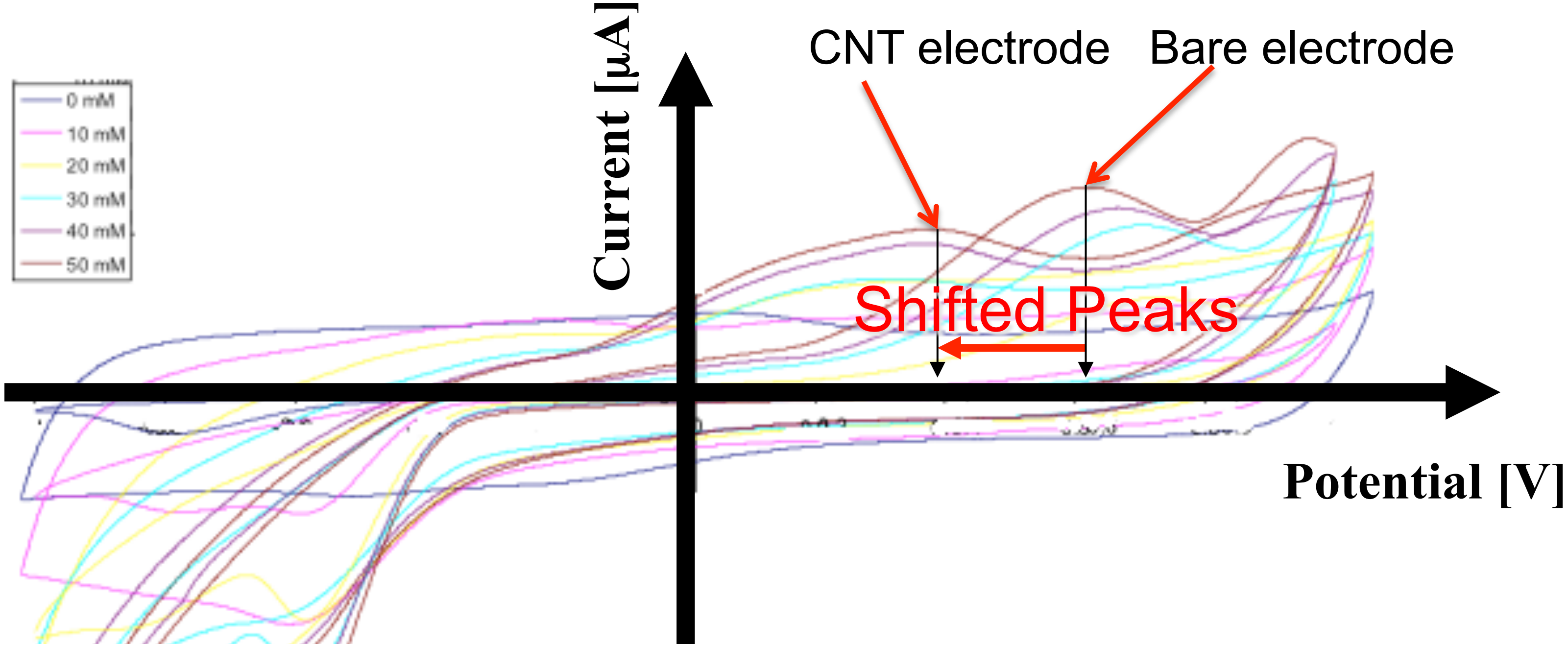

Table 3
Largely evident Nernst effect on H_2O_2.

H_2O_2 Concentration	Bare		CNT	
	Current (μA)	*Potential (mV)*	*Current (μA)*	*Potential (mV)*
10 mM	3.9 ± 0 1	706±0.4	9.1+1.6	174 ± 2.7
20 mM	23.7 ± 0.1	682±0.3	37.0 ± 1.9	204 ± 0.8
30 mM	49.5 ± 0.2	665±0.3	70.5 ± 1.3	230 ± 0.8
40 mM	55.0 ± 0.2	623±0.4	103.5 ± 2.4	291 ± 0.5
50 mM	64.4 ± 0.3	572±0.3	115.0 ± 2.7	284 ± 0.5

S. Carrara et al. / Electrochimica Acta 128 (2014) 102–112

Nernst Effect on O_2 reduction

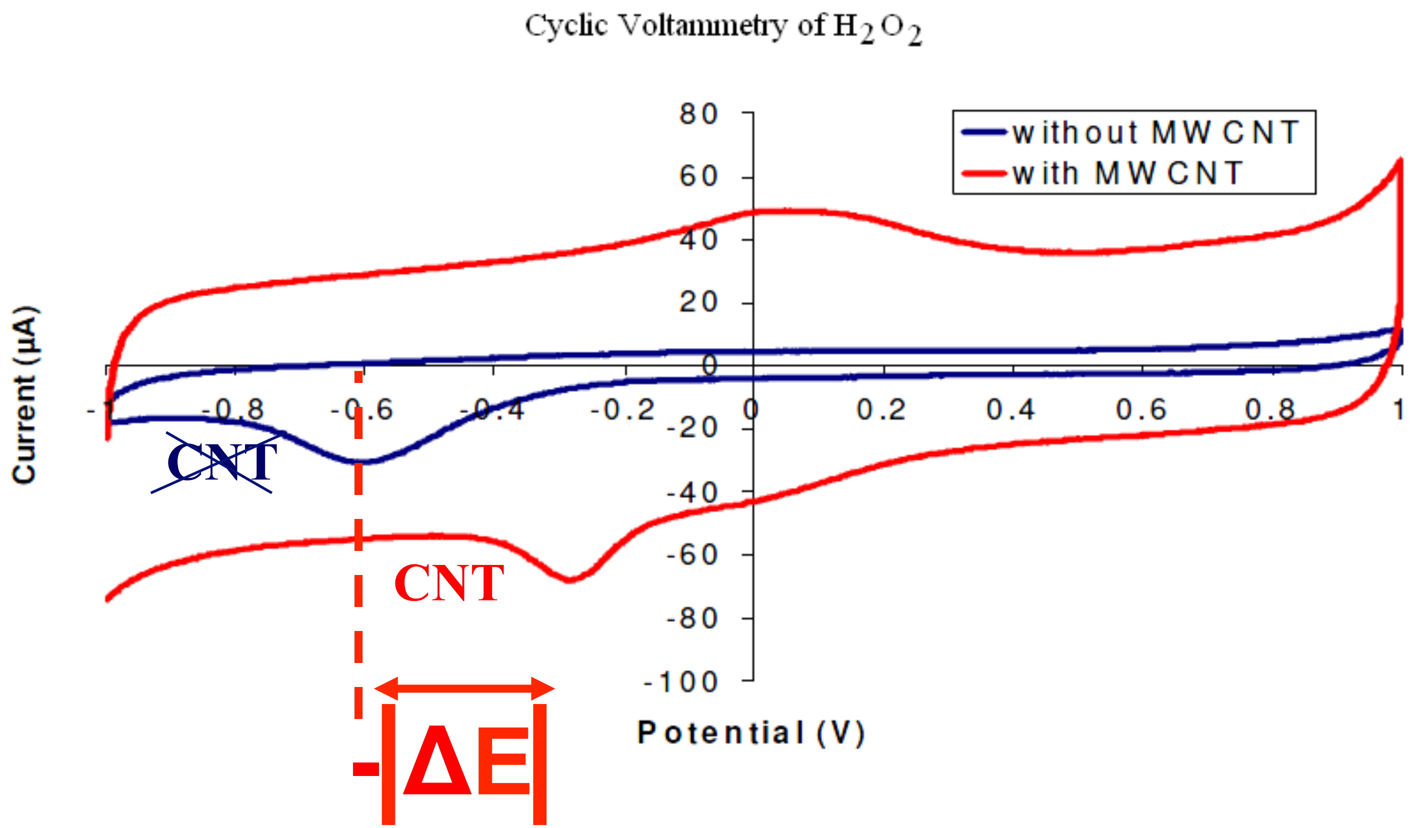

The peak potential is shifted toward lower potentials in case of electrons-transfer is mediated by carbon nanotubes

Nernst Effect on P450 2B4

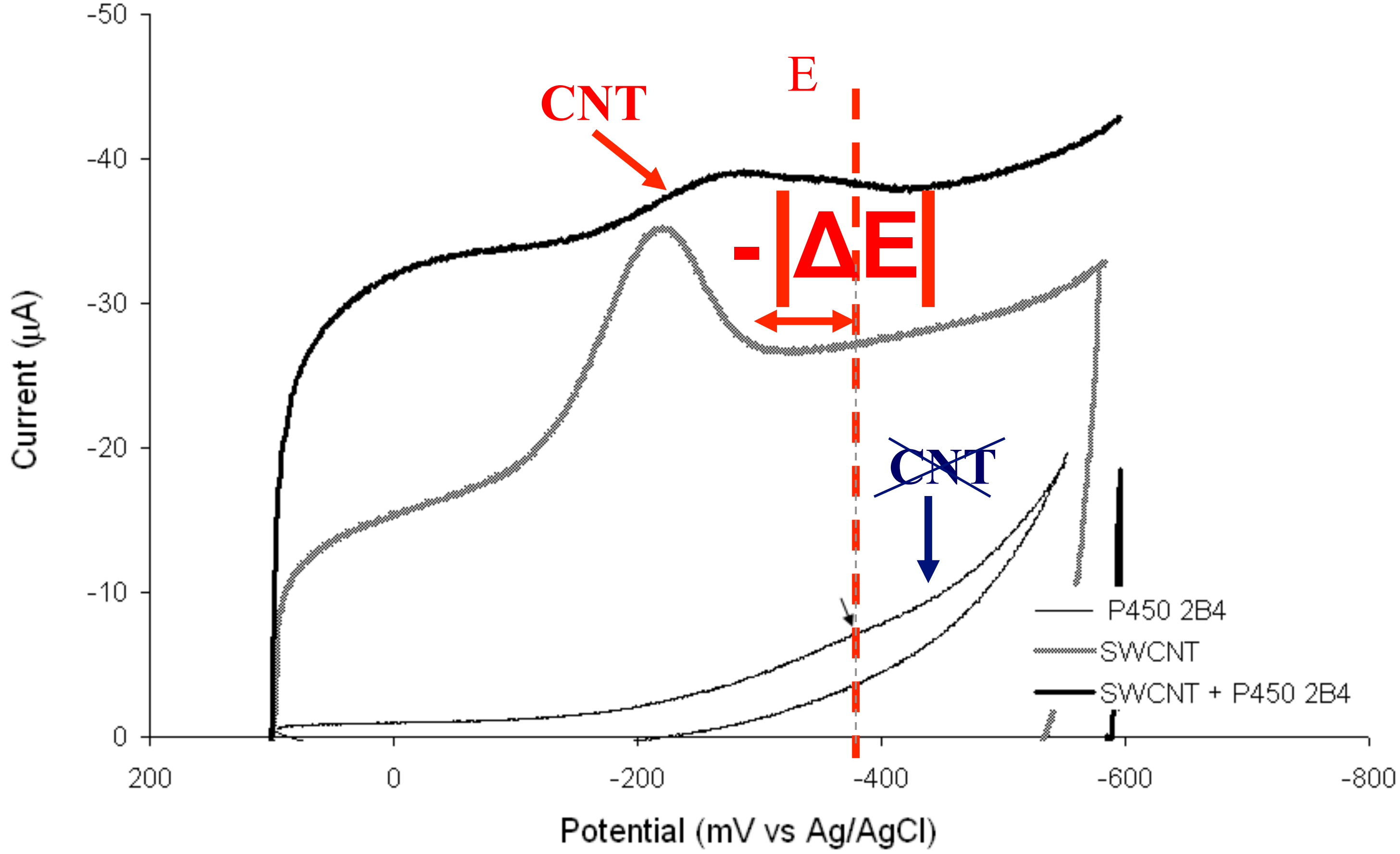

The peak potential is shifted toward lower potentials in case of electrons-transfer is mediated by carbon nanotubes

Nernst effect on different P450s

Table 1
Randle-Sevcick effect and clear Nernst effect on Cyclophosphamide by P450 2B6.

Cyclophosphamide Concentration	Bare		CNT	
	Current (μA)	*Potential (mV)*	*Current (μA)*	*Potential (mV)*
1 mM	0.51 ± 0.01	-302.1 ± 1.9	0.64 ± 0.01	-285.0 ± 3.8
2 mM	0.50 ± 0.01	-299.7 ± 1.9	0.77 ± 0.00	-280.1 ± 1.1
3 mM	0.52 ± 0.01	-294.8 ± 1.7	1.03 ± 0.01	-265.5 ± 3.6
4 mM	0.53 ± 0.01	-299.7 ± 2.0	1.51 ± 0.01	-265.5 ± 3.8
5 mM	0.51 ± 0.01	-298.5 ± 2.6	1.99+0.01	-248.4 ± 3.6

Table 2
Randle-Sevčick effect and clear Nernst effect on Cyclophosphamide by P450 3A4.

Cyclophosphamide Concentration	Bare		CNT	
	Current (μA)	*Potential (mV)*	*Current (μA)*	*Potential (mV)*
1 mM	0.82±0.01	-288.6±3.8	1.54±0.01	-221.1 ± 7.7
2 mM	0.82±0.01	-279.7±2.8	1.59±0.02	-220.5 ± 8.7
3 mM	0.84±0.01	-272.7±3.1	1.60±0.01	-222.1 ± 7.3
4 mM	0.86±0.01	-264.4±2.9	2.12±0.01	-225.7 ± 4.6
5 mM	0.85±0.01	-262 2±3 1	3 02±0.01	-223.6 ± 4.6

S. Carrara et al. / Electrochimica Acta 128 (2014) 102–112

Peak position by Nernst

The position (E) of the reduction and oxidation peaks of a specie is related to the standard potential (E_0) and to the concentration of species in oxidized and reduced forms by the well-known Nernst equation

$$E_{Nerst} = E_0 + \frac{RT}{nF} \ln \left[\frac{C_o}{C_R} \right]$$

Peak position by Thin-layer effect

However, the semi-infinite planar diffusion model does not work when dealing with nano-structuring. In this case, the phenomenon is more accurately explained by thin-layer effects, which foresees a fully irreversible electron transfer system as driven by

$$E = E_{Nerst} + \frac{ET}{\alpha F} \ln\left(\frac{\alpha F \upsilon}{RTlk_0}\right)$$

l is the thickness of the thin layer α and k_0 are the usual transfer coefficient and standard heterogeneous rate constant, respectively

CNTs contribution to Layering Effects

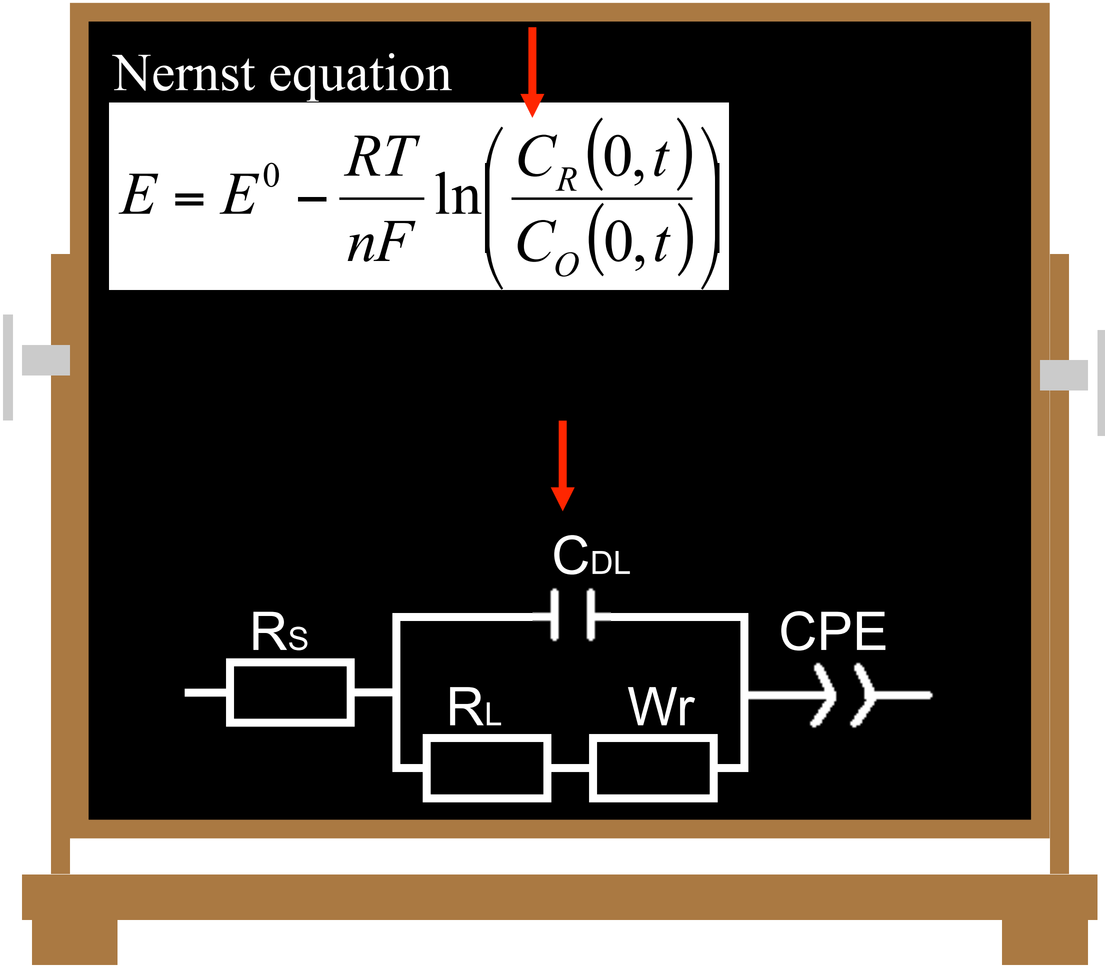

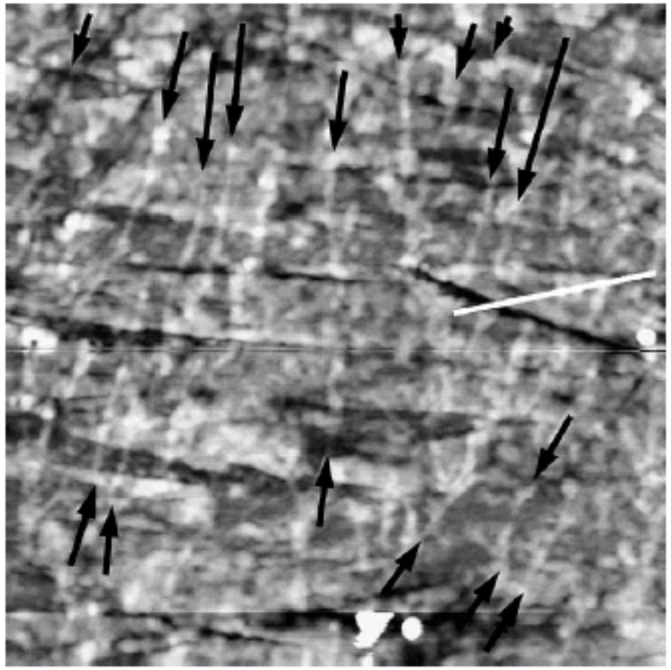

S. Carrara et al. / Sensors and Actuators B 109 (2005) 221–226

Randle Model

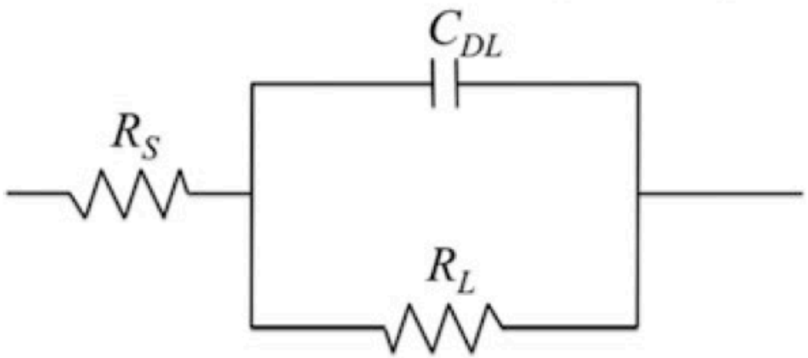

$$\underline{Z}_{Randle} = R_S + \underline{Z}_C \, // R_L$$

$$\underline{Z}_{//} = \frac{R_L}{j\omega C_{DL} R_L + 1}$$

Equivalent circuits of the Bio/CMOS interface

Cole-Cole Plots (or **Nyquist Plots**)

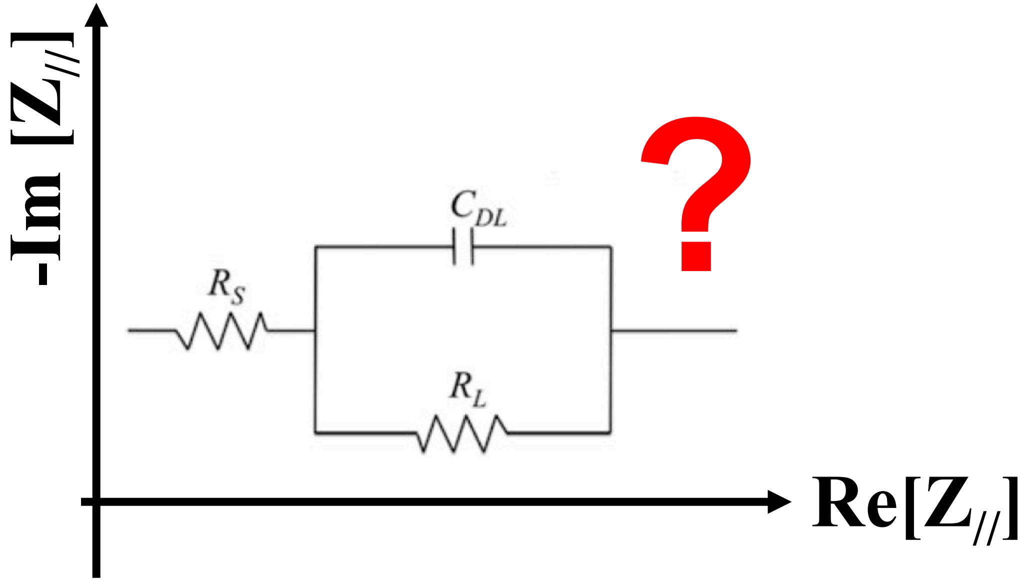

Cole-Cole plots are parametric plots of the frequency response of the interface

Cole-Cole Plots (or **Nyquist Plots**)

$$\underline{Z}_{//} = \underline{Z}_C \,//\, R_L = \frac{R_L}{\left(1 + j\omega C R_L\right)}$$

$$\underline{Z}_{//} = \frac{R_L}{1 + j\omega R_L C} = \frac{R_L(1 - j\omega C)}{1 + (\omega R_L C)^2}$$

$$\underline{Z}_{//} = R_{//} + jX_{//}, \, with \begin{cases} y = -X_{//} = \dfrac{\omega R_L C}{1 + (\omega R_L C)^2} \\ x = R_{//} = \dfrac{R_L}{1 + (\omega R_L C)^2} \end{cases}$$

Cole-Cole plots are parametric plots of the frequency response of the interface

Cole-Cole Plots (or **Nyquist Plots**)

$$\left|\underline{Z}_{//}\right|^2 = \frac{R_L^2[1+(\omega R_L C)^2]}{[1+(\omega RLC)^2]^2} = \frac{R_L^2}{[1+(\omega RLC)^2]} = R_L R_{//}$$

$$Z_{//}^2 = R_{//}^2 + X_{//}^2 = R_L R_{//} \longrightarrow R_{//}^2 + X_{//}^2 - R_L R_{//} = 0$$

$$X_{//}^2 + \left(R_{//} - \frac{R_L}{2}\right)^2 - \left(\frac{R_L}{2}\right)^2 = 0$$

That's a circle with centre in the position (*R_L/2;0*) and radius equal to *R_L/2* !!!

Cole-Cole plots are parametric plots of the frequency response of the interface

Cole-Cole Plots (or Nyquist Plots)

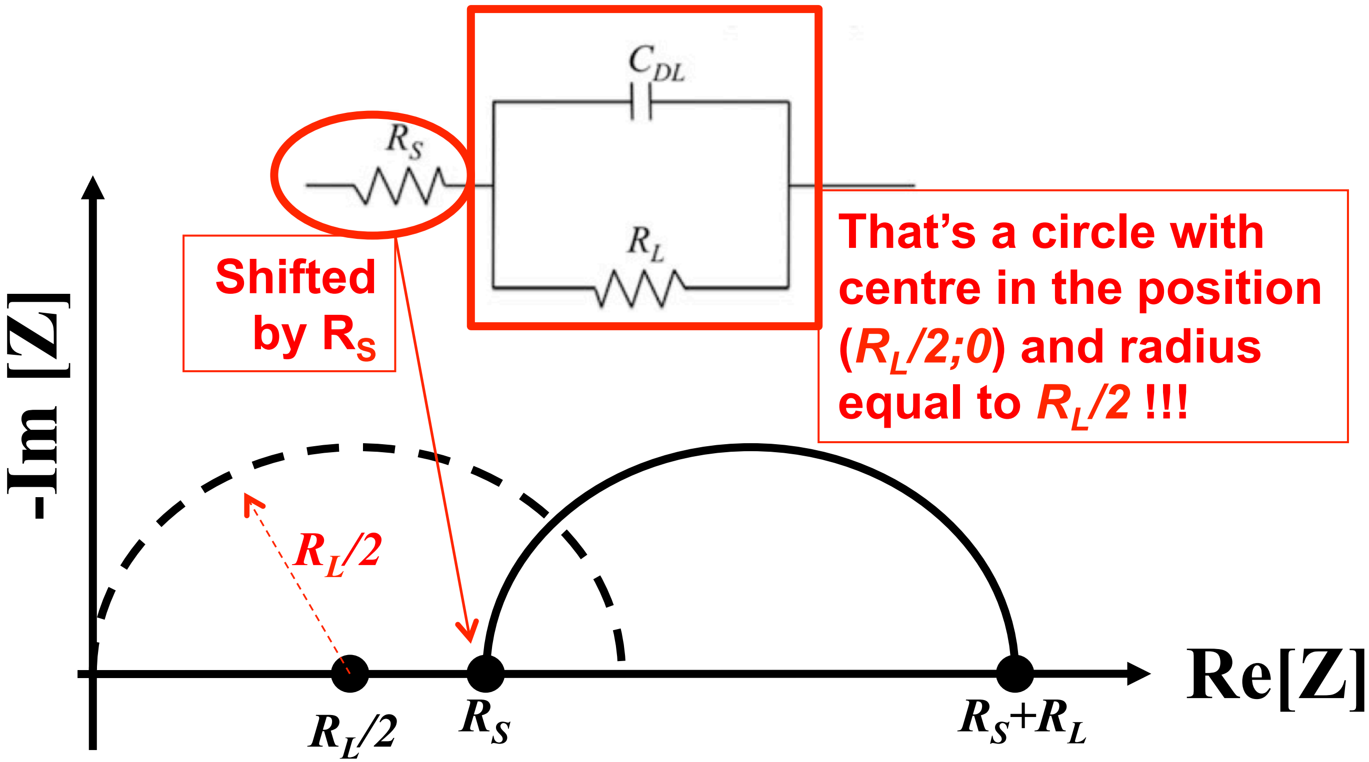

Cole-Cole plots are parametric plots of the frequency response of the interface

Cole-Cole Plots (or **Nyquist Plots**)

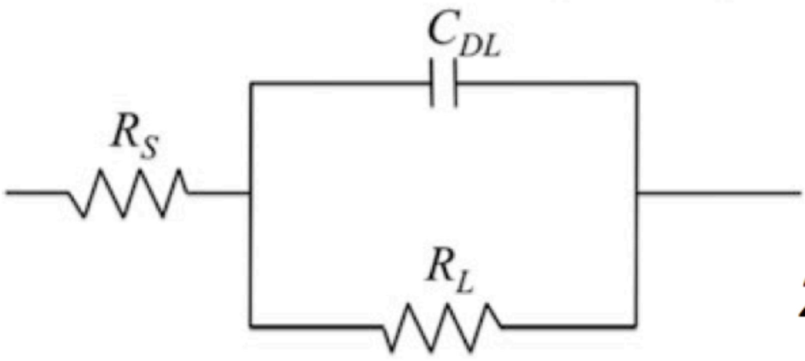

$$Z_{//} = \frac{R_L}{j\omega C_{DL} R_L + 1} \cdot \frac{1 - j\omega C_{DL} R_L}{1 - j\omega C_{DL} R_L}$$

$$Z_{//} = \frac{R_L}{1 + (\omega C_{DL} R_L)^2} - j\,\frac{\omega C_{DL} R_L^2}{1 + (\omega C_{DL} R_L)^2}$$

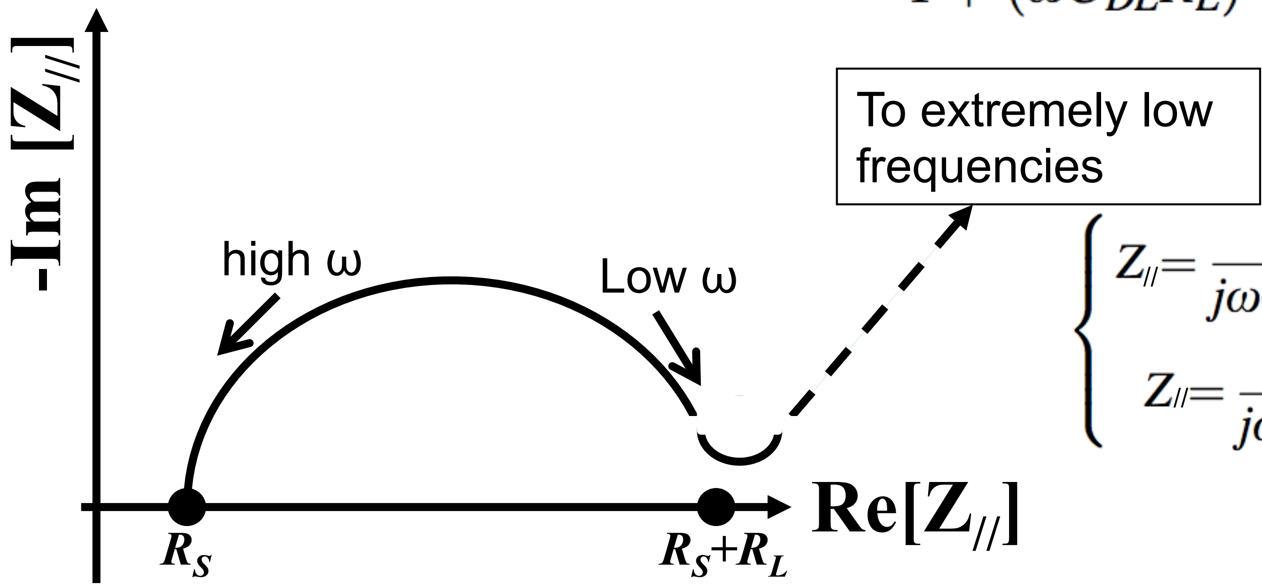

$$\begin{cases} Z_{//} = \dfrac{R_L}{j\omega C_{DL} R_L + 1} \xrightarrow{\omega \to 0} R_L \\ Z_{//} = \dfrac{R_L}{j\omega C_{DL} R_L + 1} \xrightarrow{\omega \to \infty} 0 \end{cases}$$

The interface model is well described by the Nyquist plot

CNTs contribution to Layering Effects

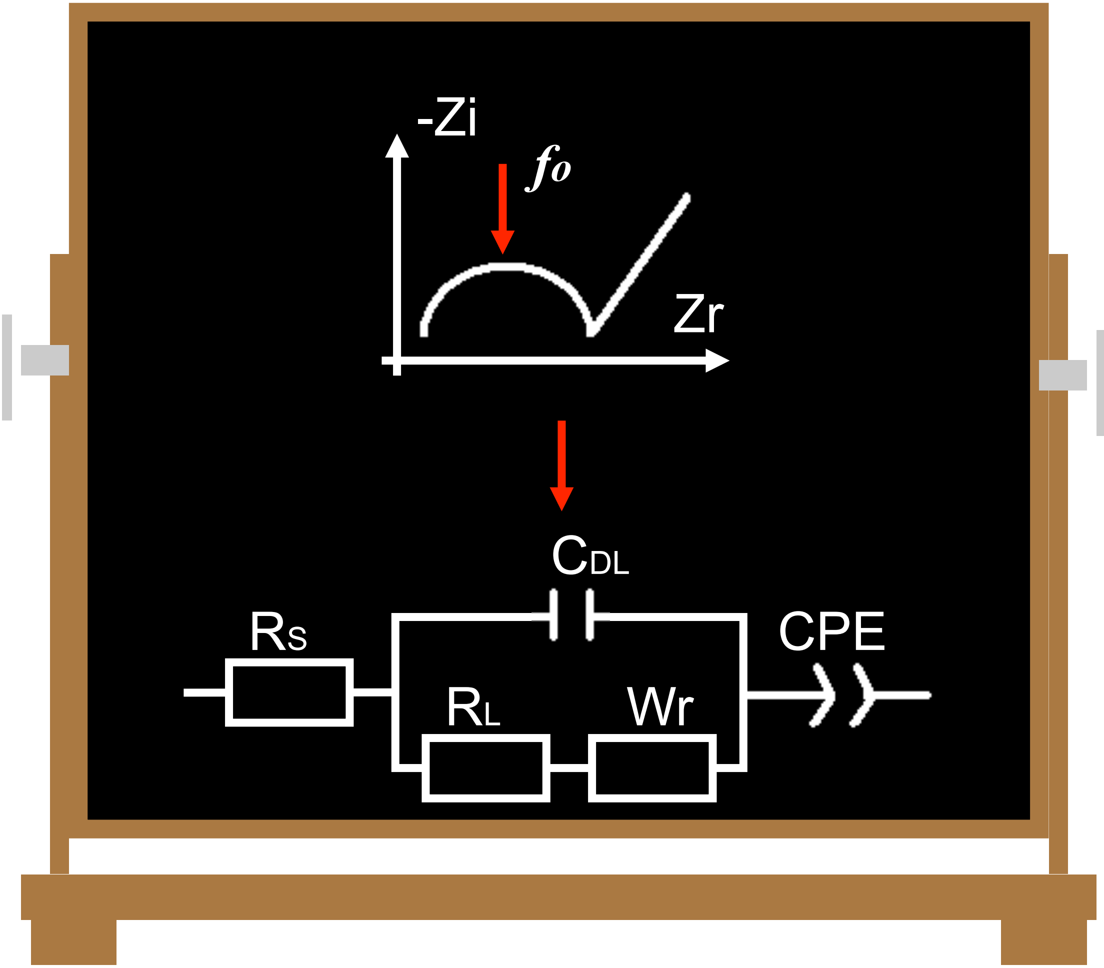

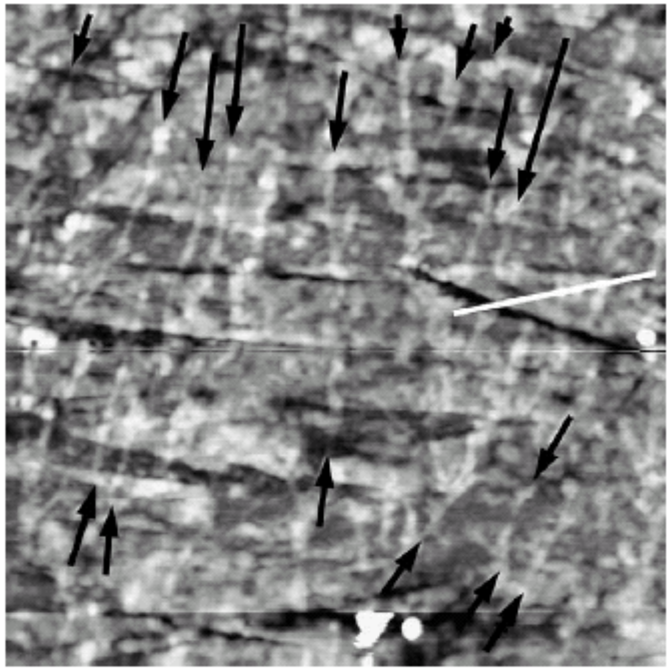

S. Carrara et al. / Sensors and Actuators B 109 (2005) 221–226

Poly-(ortho)-anisidine (POAS)

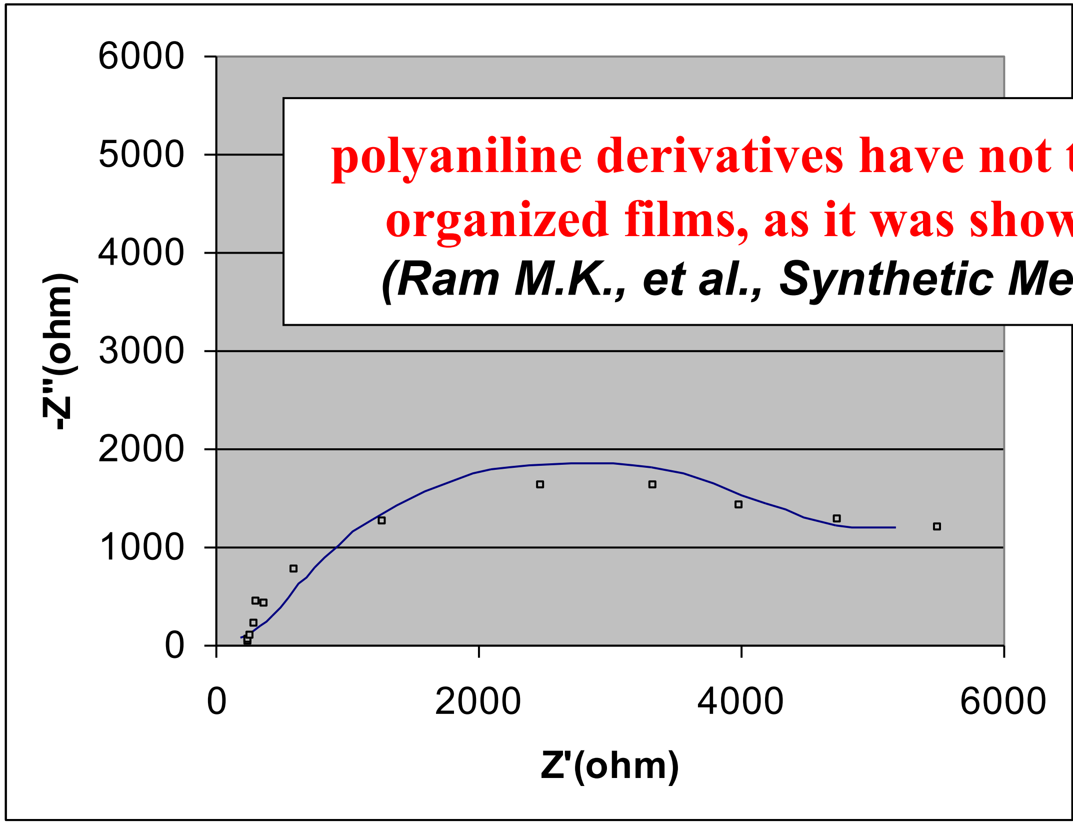

polyaniline derivatives have not the tendency to form well organized films, as it was shown by AFM microscopy

(Ram M.K., et al., Synthetic Metals 100(1999) 249-259)

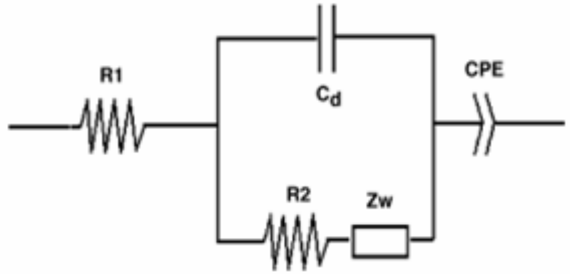

Nyquist impedance diagram of a pure POAS film

Conducting Polymer + Carbon Particles

Consistent with the Lundberg Theory of conducting mixtures

(B.Lundberg, B.Sundqvist, J.Appl.Phys. 60(1986) 1074-1079)

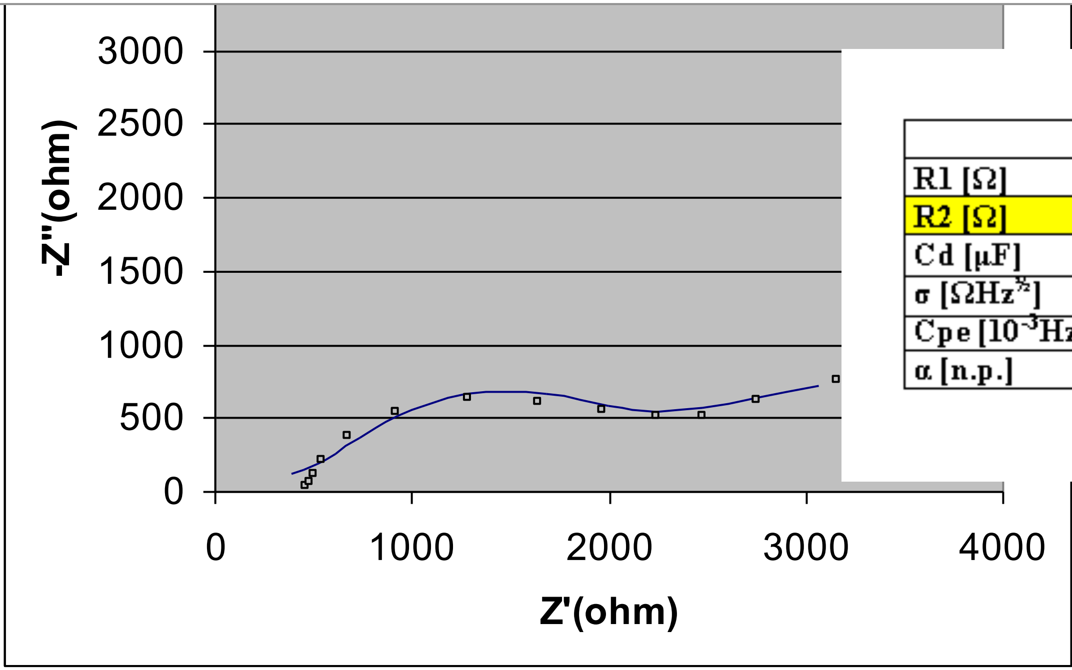

	POAS	POAS+CB
R1 [Ω]	46	64
R2 [Ω]	3165	869
Cd [μF]	32.7	23.3
σ [$\Omega Hz^{½}$]	353	252
Cpe [$10^{-3} Hz^{-\alpha}/\Omega$]	0.57	0.49
α [n.p.]	0.298	0.207

decrease of the charge transfer resistance

Nyquist impedance diagram of a POAS film. Experimental data are showed by boxes. Data are acquired in the frequency range from 1KHz down to 100mHz. The solid line shows the best fitting

Conducting Polymer + Multi Walled CNTs

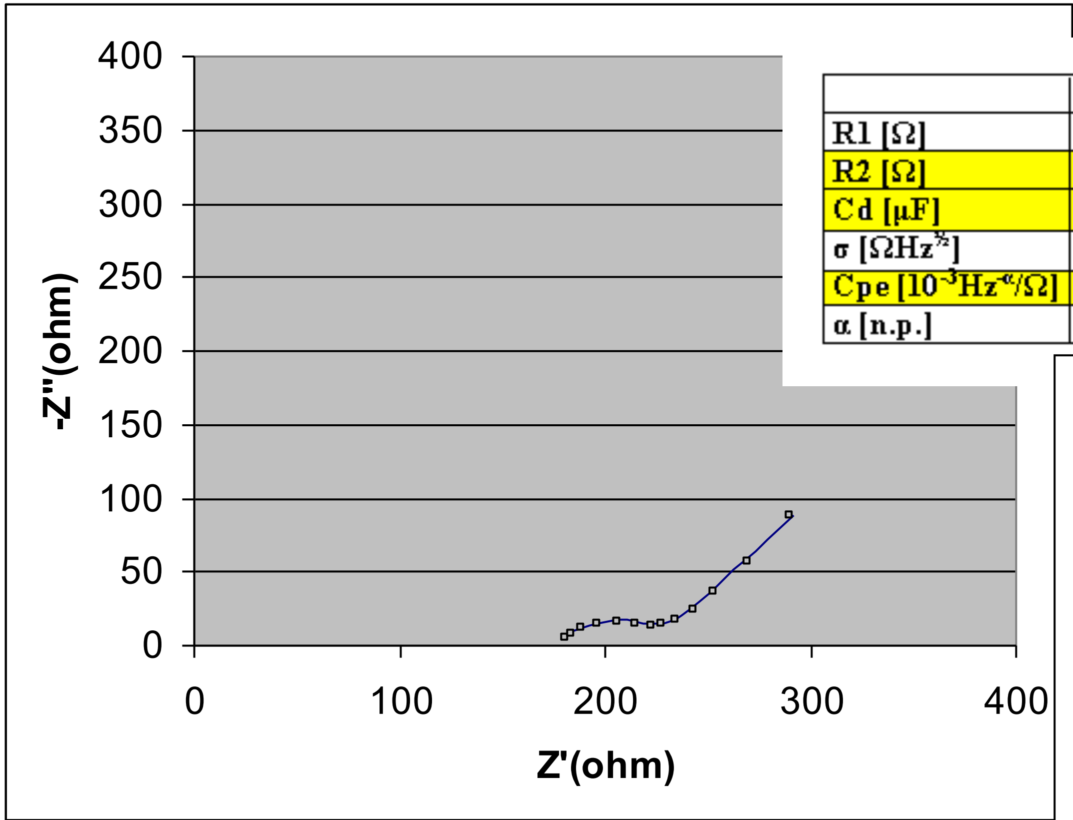

S.Carrara et al., Sensors and Actuators B: Chemicals 109 (2005) 221-226

	POAS	POAS+NT
R1 [Ω]	46	173
R2 [Ω]	3165	50
Cd [μF]	32.7	117.1
σ [$\Omega Hz^{1/2}$]	353	215
Cpe [$10^{-3} Hz^{\alpha}/\Omega$]	0.57	11.68
α [n.p.]	0.298	.575

Pure electrostatic attraction in the double layer and faradic reaction are responsible for the super-capacitance phenomena in Carbon Nanotubes structures

Pan et al., Chem. Mater., Vol. 19, No. 25, 2007

- Nyquist impedance diagrams of a POAS film synthesized with Carbon Nanotubes. Experimental data are showed by boxes. Data are acquired in the frequency range from 1KHz down to 100 mHz. The solid line shows the best fitting

Cottrell Effects on H_2O_2

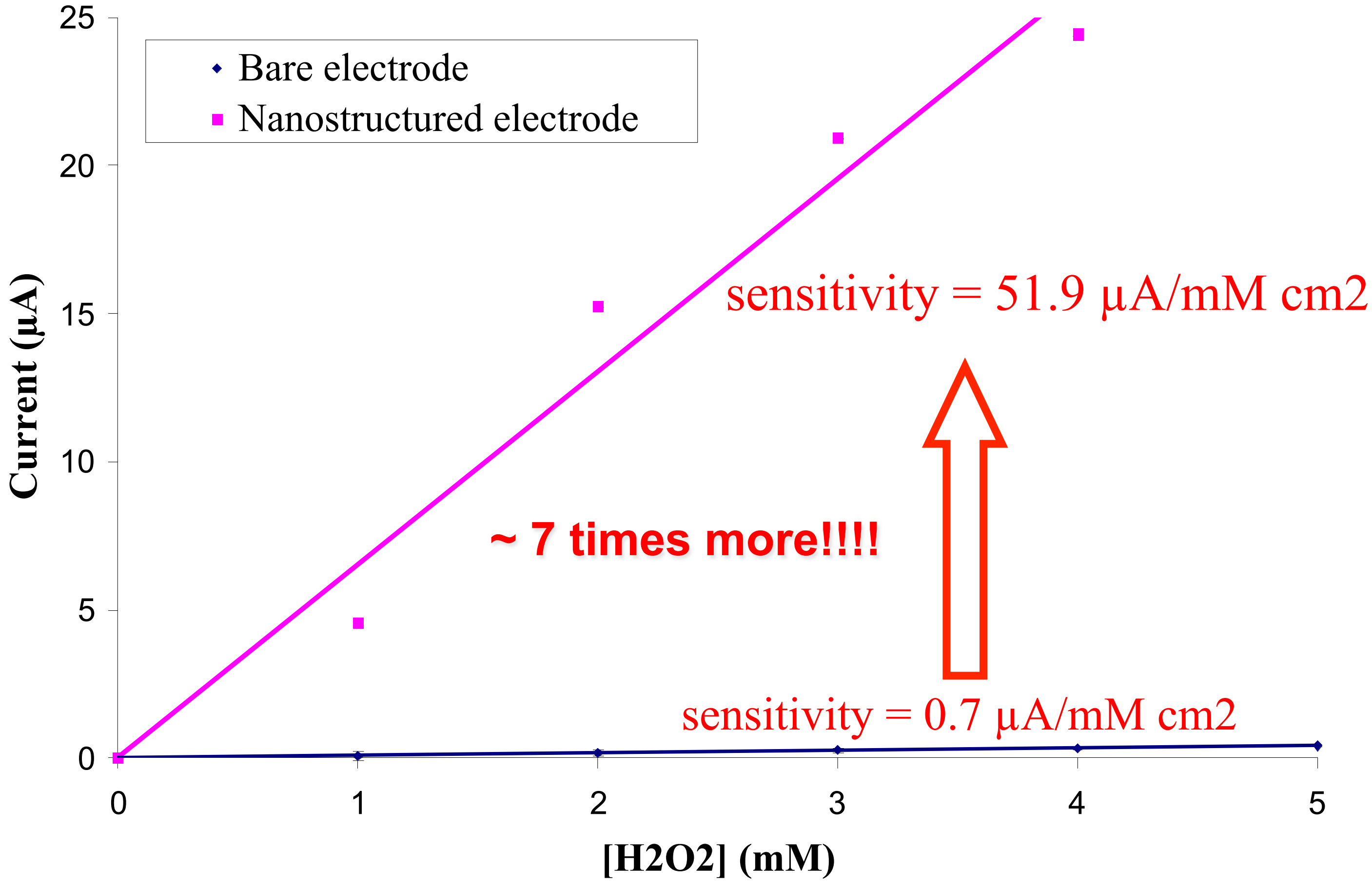

Peroxide Detection

TABLE I

SENSITIVITY VALUES FROM LITERATURE

Methods	Sensitivity
Au-Nafion®- TNTs [11]	0.24 $\mu A\ mM^{-1}\ cm^{-2}$
Polypyrrole - polyanion/PEG [12]	0. 5 $\mu A\ mM^{-1}\ cm^{-2}$
MWCNT-chitosan [13]	8 3 $\mu A\ mM^{-1}\ cm^{-2}$
chitosan/PVI-Os/CNT [9]	19.7 $\mu A\ mM^{-1}\ cm^{-2}$

2 order of magnitude!!!

[9] X. Cui, *Biosensors and Bioelectronics*, vol. 22, pages 3288-3292, 2007

[11] M. Yang, *Nanotechnology*, vol. 19, page 075502, 2008

[12] W.J. Sung, *Sensors and Actuators B*, vol. 114, pages 164-169, 2006

[13] Y. Tsai, *Sensors and Actuators B*, vol. 125, pages 474-481, 2007

The peroxide detection is highly improved by using carbon nanotubes

Cottrell effect on Glucose Oxidase

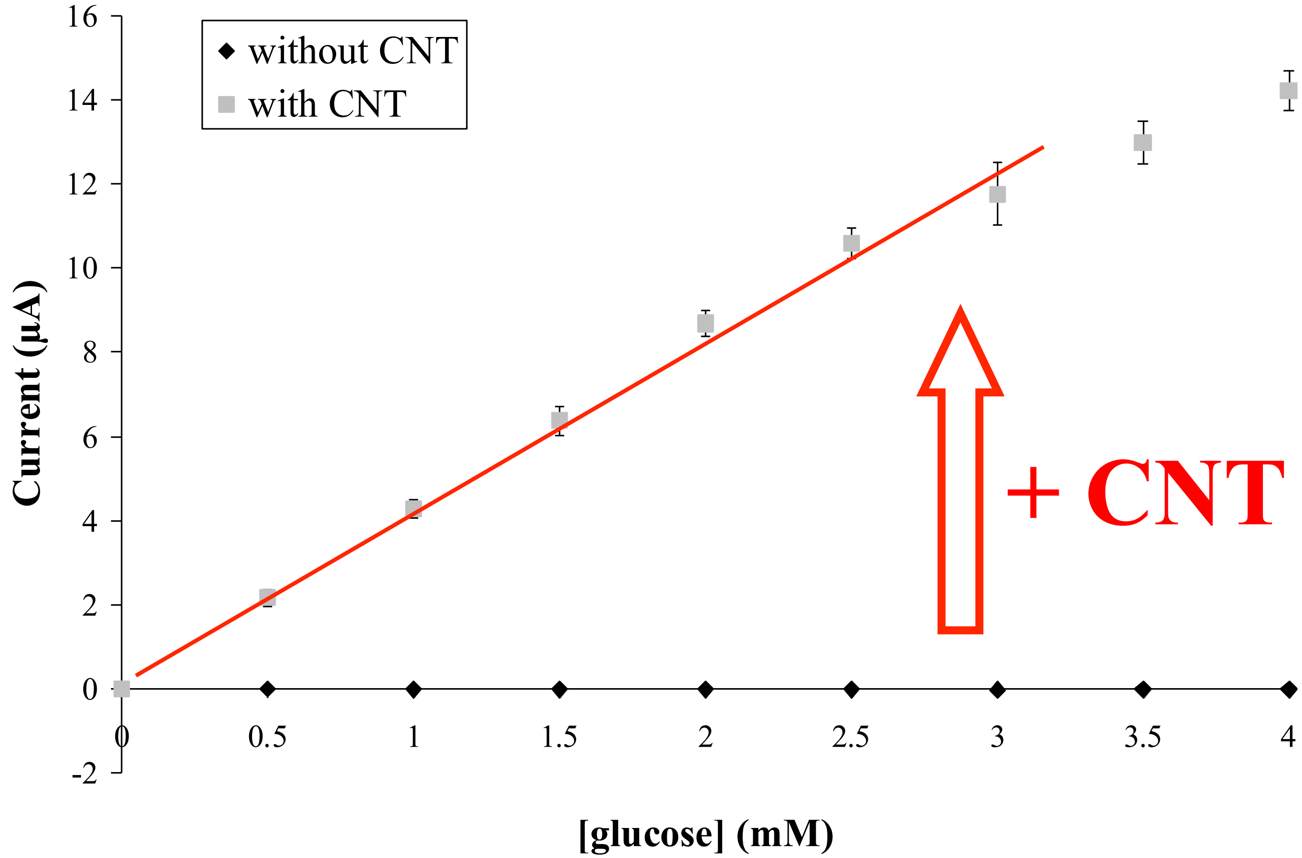

Cottrell effect on Lactate Oxidase

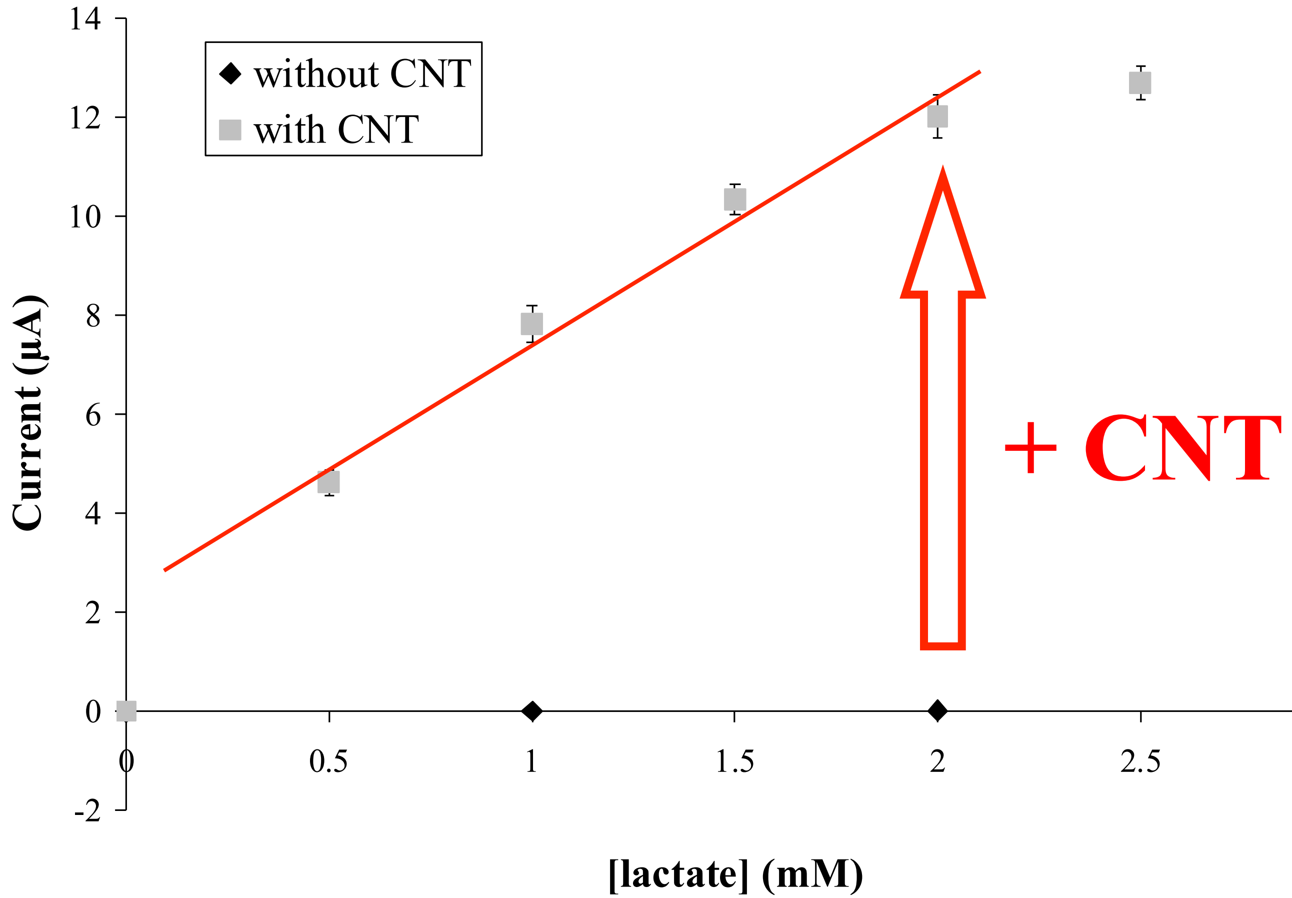

Cottrell effect on P450 2B4

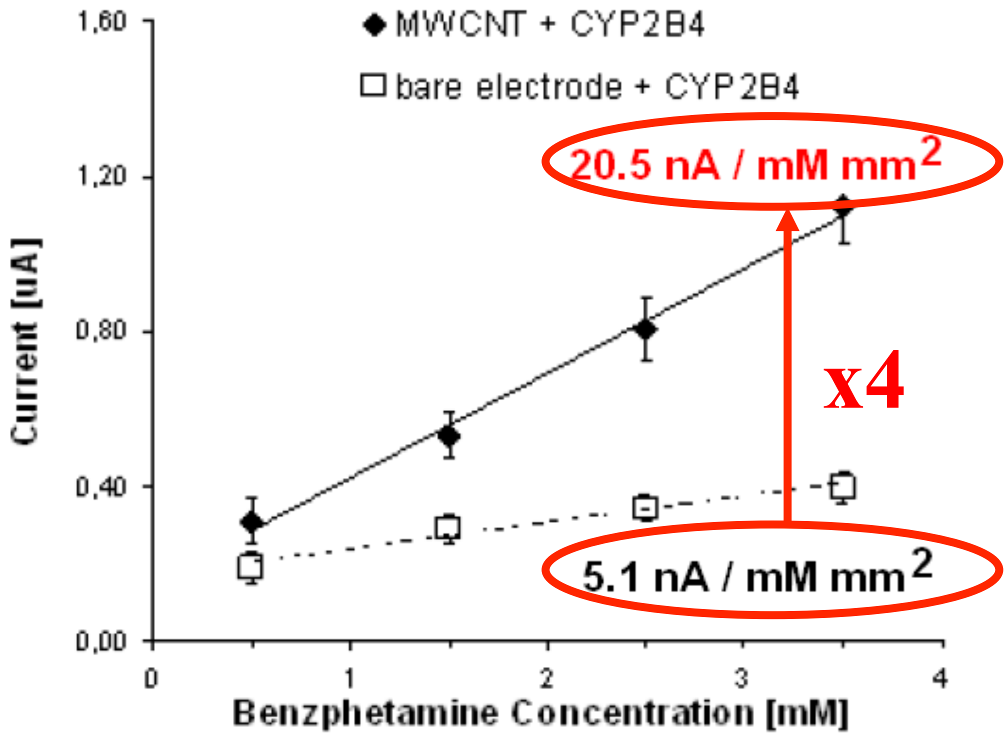

S. Carrara et al., Conference Proceedings of IEEE CME2009, Tempe (US), 9-11, April, 2009

P450 2B4 performance in detecting Benzphetamine is enhanced by a factor 4x by using MWCNT

Increased Sensitivity by different techniques

		Sensitivity * [μA/(mM*cm^2)]	Limit of Detection * (LOD) [μM]
			* on Glucose detection
DROP CASTING	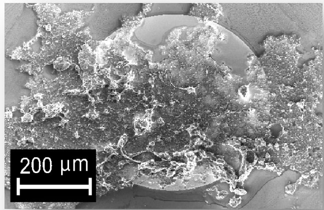	27.7 ± 0.1	73 ± 1
MICRO SPOTTING	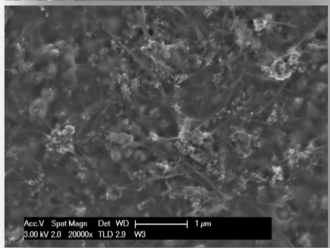	0.46 ± 2	115 ± 1
ELECTRO DEPOSITION	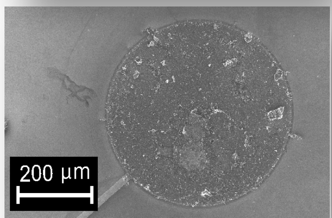	63 ± 15	8 ± 2
CVD growth	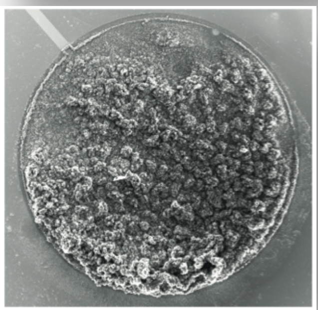	111.2 ± 0.3 (5703 ± 566	0.745 ± 0.005 3.5 ± 1.3) #

on Uric Acid detection

Randles-Sevçik Effect on P450

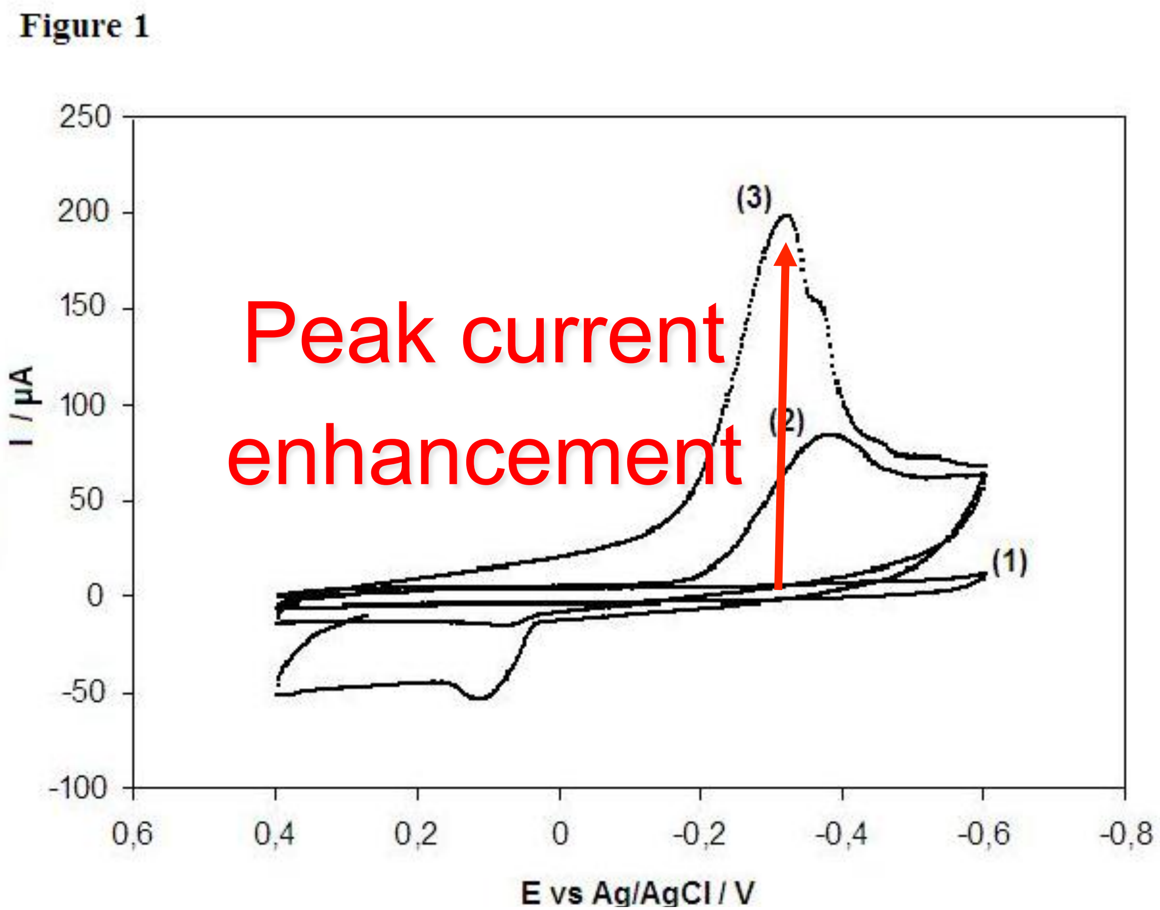

S. Carrara et al. / Biosensors and Bioelectronics 24 (2008) 148–150

The Peak Current is larger when the P450 11A1 Activity is mediated by Multi Walled Carbon Nanotubes

Randles-Sevçik effect on different P450s

Table 1
Randle-Sevcick effect and clear Nernst effect on Cyclophosphamide by P450 2B6.

Cyclophosphamide Concentration	Bare		CNT	
	Current (μA)	*Potential (mV)*	*Current (μA)*	*Potential (mV)*
1 mM	0.51 ± 0.01	-302.1 ± 1.9	0.64 ± 0.01	-285.0 ± 3.8
2 mM	0.50 ± 0.01	-299.7 ± 1.9	0.77 ± 0.00	-280.1 ± 1.1
3 mM	0.52 ± 0.01	-294.8 ± 1.7	1.03 ± 0.01	-265.5 ± 3.6
4 mM	0.53 ± 0.01	-299.7 ± 2.0	1.51 ± 0.01	-265.5 ± 3.8
5 mM	0.51 ± 0.01	-298.5 ± 2.6	1.99+0.01	-248.4 ± 3.6

Table 2
Randle-Sevčick effect and clear Nernst effect on Cyclophosphamide by P450 3A4.

Cyclophosphamide Concentration	Bare		CNT	
	Current (μA)	*Potential (mV)*	*Current (μA)*	*Potential (mV)*
1 mM	0.82±0.01	-288.6±3.8	1.54±0.01	-221.1 ± 7.7
2 mM	0.82±0.01	-279.7±2.8	1.59±0.02	-220.5 ± 8.7
3 mM	0.84±0.01	-272.7±3.1	1.60±0.01	-222.1 ± 7.3
4 mM	0.86±0.01	-264.4±2.9	2.12±0.01	-225.7 ± 4.6
5 mM	0.85±0.01	-262 2±3 1	3 02±0.01	-223.6 ± 4.6

S. Carrara et al. / Electrochimica Acta 128 (2014) 102–112

Randles-Sevçik effect on P450 3A4

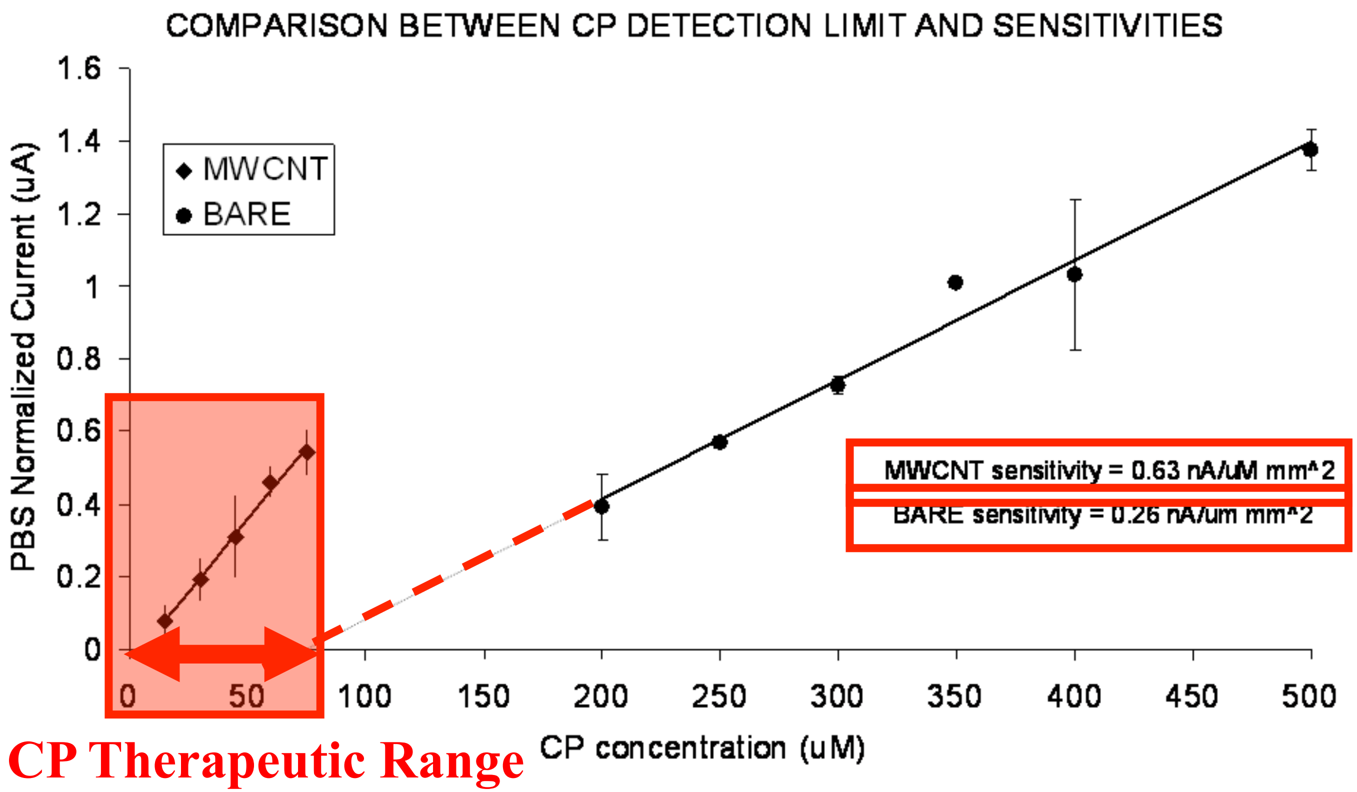

S. Carrara et al. / Biosensors and Bioelectronics 26 (2011) 3914–3919

Cyclophosphamide (CP), an anti-cancer agent, is detected by P450 3A4 in its therapeutic range

Randles-Sevçik Effect on direct redox

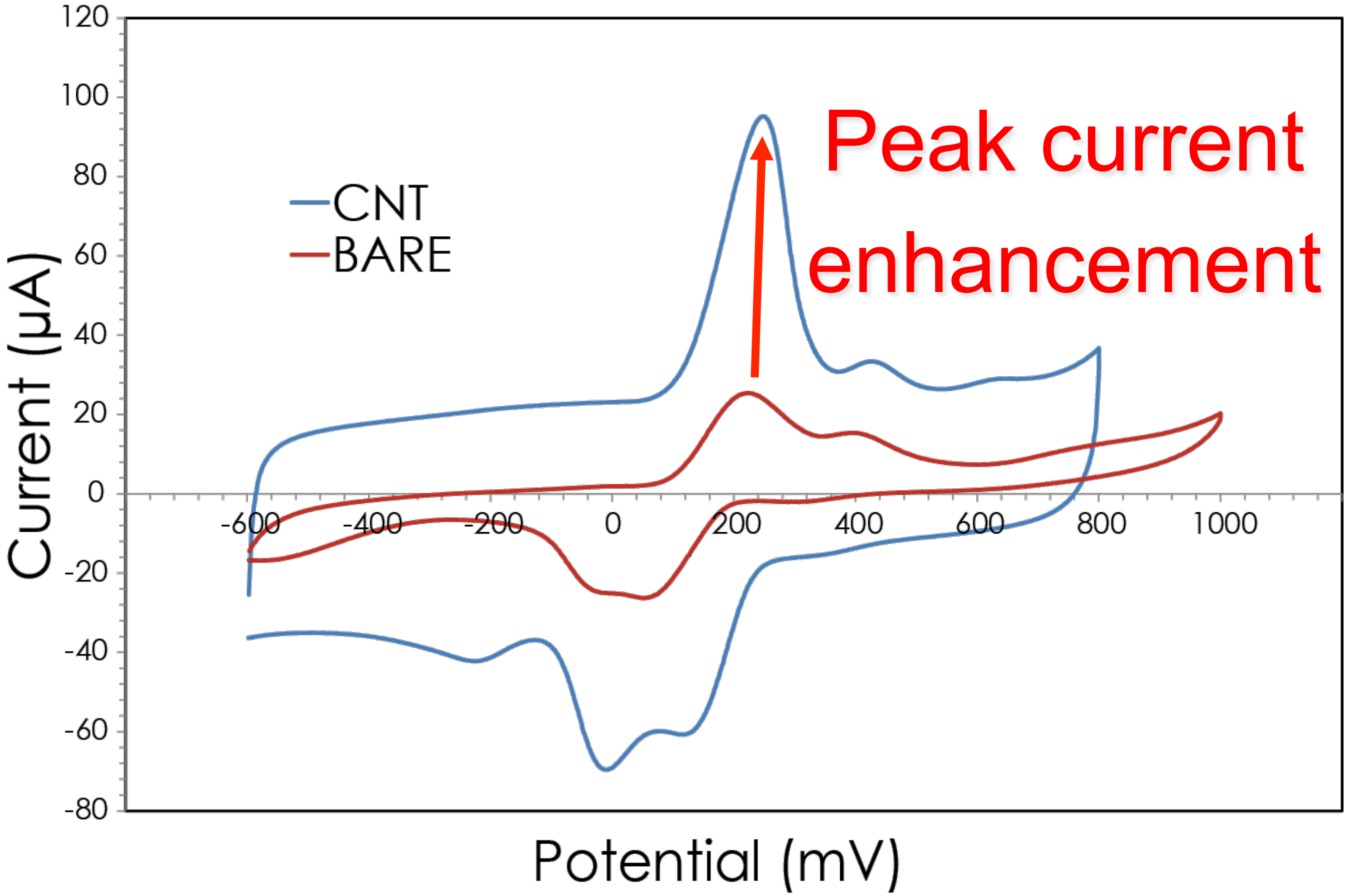

C. Baj-Rossi, S.Carrara / Sensors (2012) 6520-6537

The Peak Current is larger when the Etoposide redox is mediated by Multi Walled Carbon Nanotubes

Electron Transfer (ET) from a P450 and a Carbon Nanotube

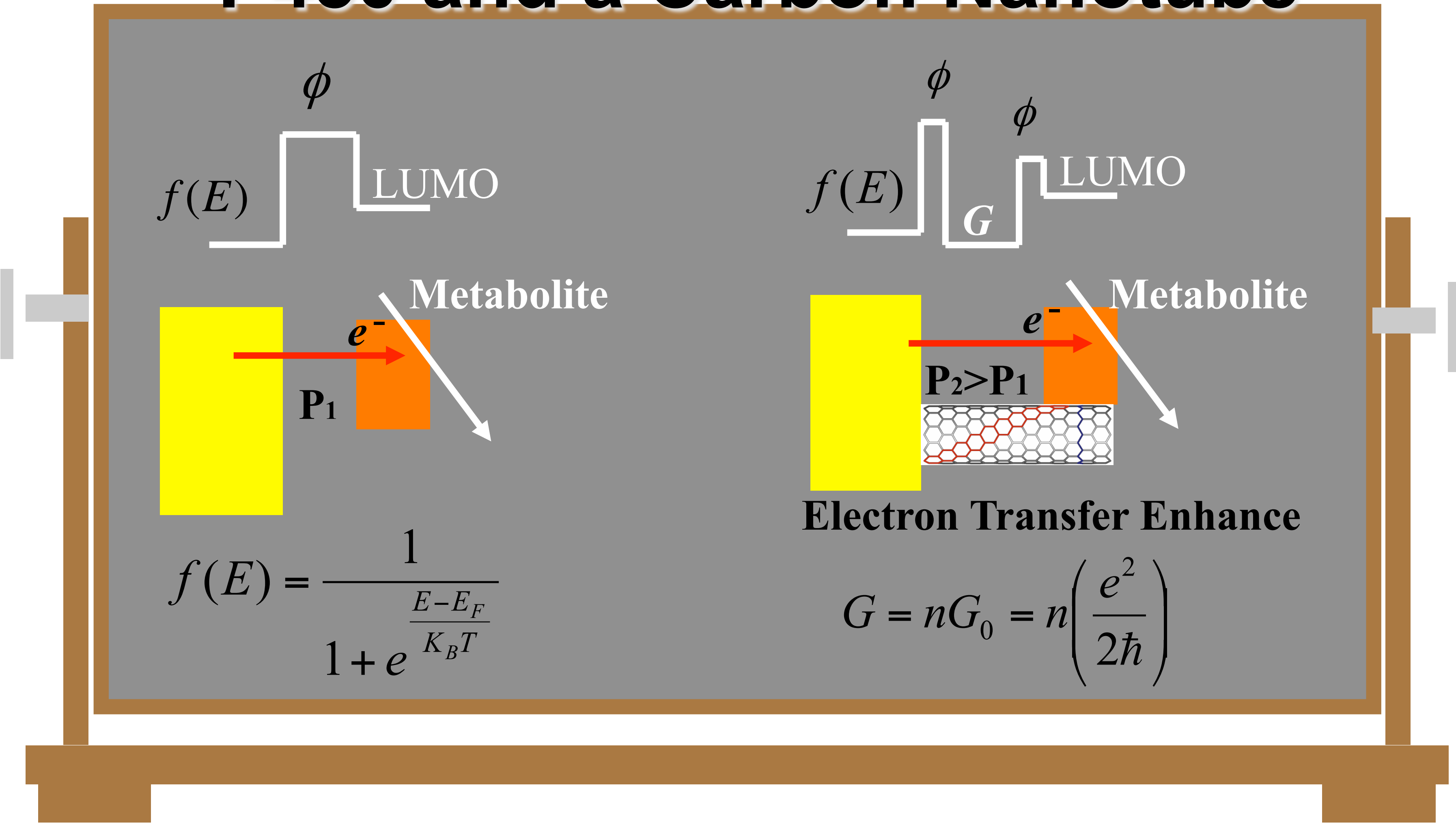

Electron Transfer

- In the case of reductions, the electrons jump from the Fermi level in the metal to the Lowest Unoccupied Molecular Orbital (LUMO) of the molecules
- In the case of oxidations, the electrons jump from the Highest Occupied Molecular Orbital (HOMO) of the molecules to the Fermi level of the metal
- In both the cases, the electrons jump to (or from) the molecular orbitals from (or to) the electrodes through a tunneling barrier, which limits the electron transfer (ET) rate

Electron Transfer Rate

$$k_{ET} = \frac{2\pi}{\hbar} V_T^2 FC$$

FC is the Franc-Condon-weighted density of states:

$$FC = \frac{1}{\sqrt{4\pi\lambda kT}} e^{-\left(\lambda kT \sqrt{-\Delta G^0 - \lambda}\right)}$$

λ is the energy arising from the increased polarity of the redox center, ΔG_o is the Gibbs free energy between the two electron states, k the Boltzmann constant.

V_T^2 is the electronic coupling between the molecules and the electrodes, depending on the tunneling barrier:

$$V_T^2 = V_0^2 e^{-\beta(\phi)d} \qquad \beta(\phi) = \sqrt{\frac{2m}{\hbar}(\phi - eV)}$$

Electron Transfer Rate

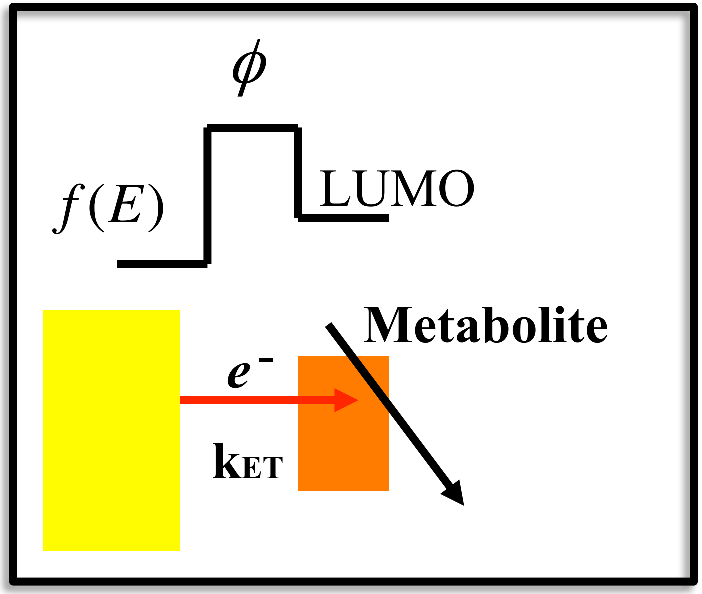

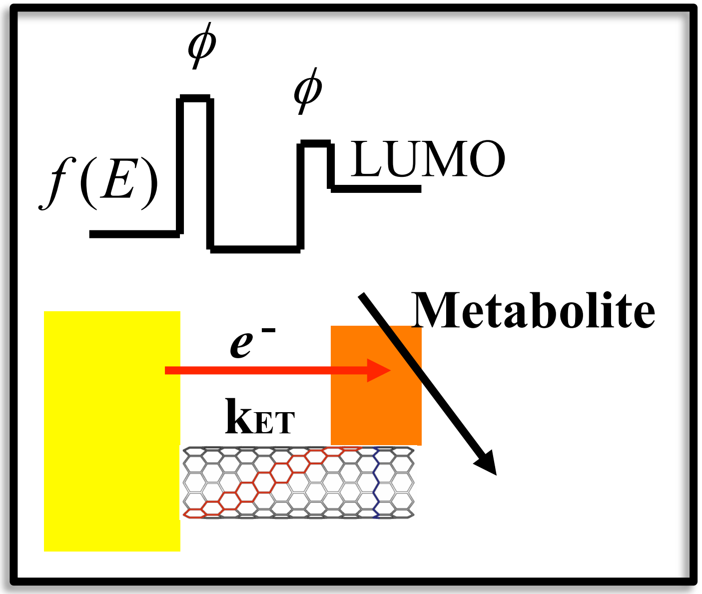

$$k_{ET} = \frac{2\pi}{\hbar} V_T^2 FC$$

$$V_T^2 = V_0^2 e^{-\beta(\phi)d}$$

$$\beta(\phi) = \sqrt{\frac{2m}{\hbar}(\phi - eV)}$$

Electron Transfer

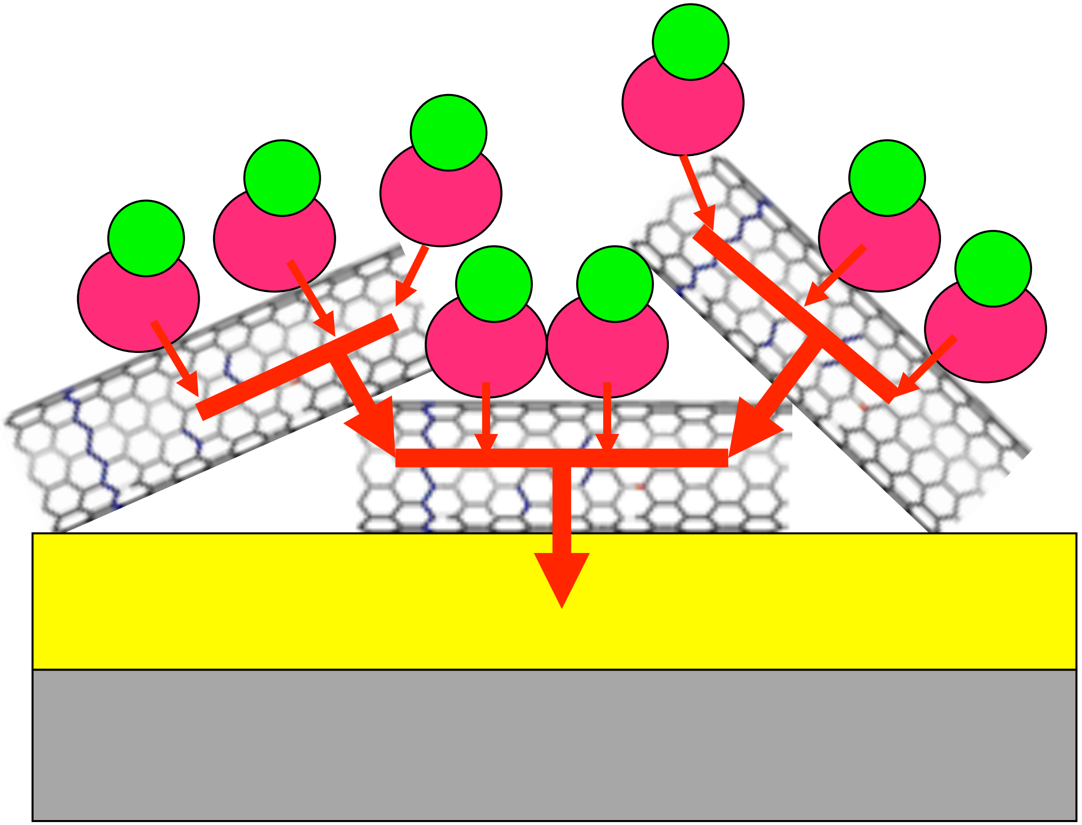

Electron transfer contributions from the CNT tips and side-walls as well

Electron emission by CNT

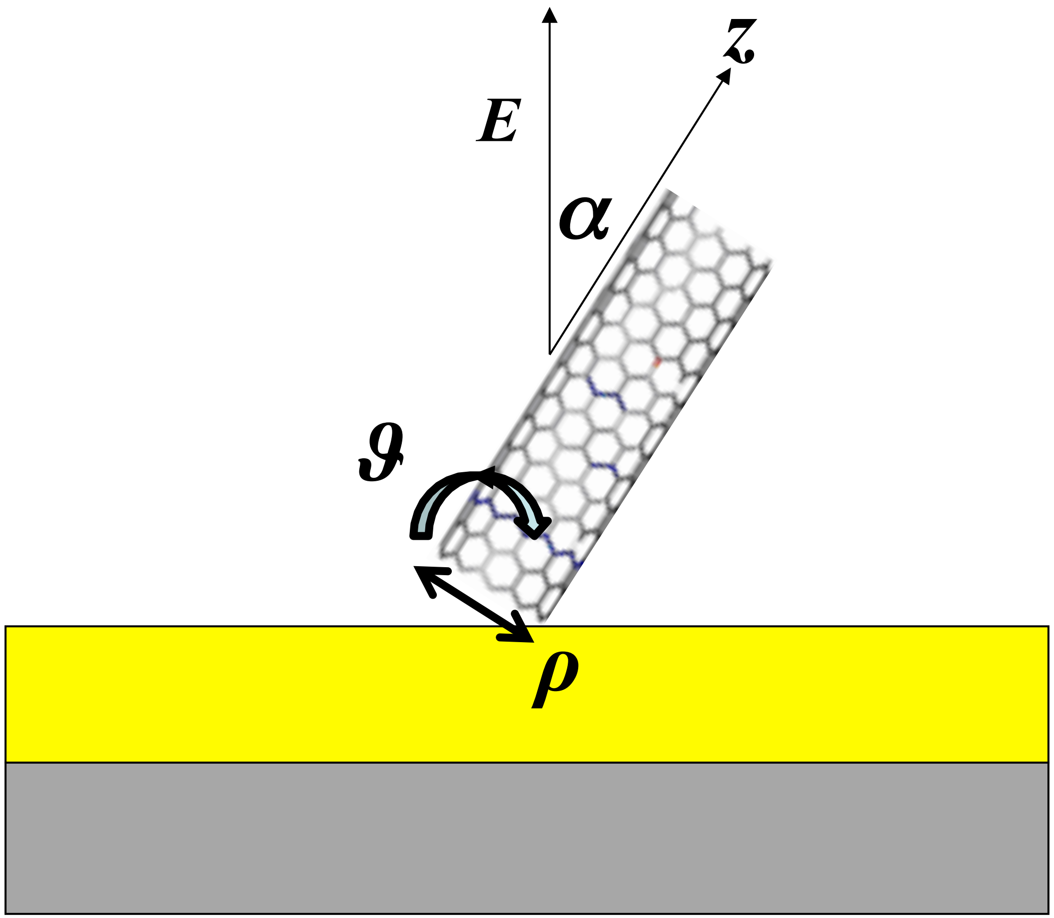

The electron emission occurs through the CNT half surface facing the anode

Electron emission by CNT

The current emitted across the surface σ obeys the Fowler–Nordheim equation considering the projection of on the normal to σ:

$$I = K_1 \sigma E_{\perp}^2 exp\left(-\frac{K_2}{E_{\perp}}\right)$$

$E_{\perp}$ is the projection of on the normal to σ, while K_1 and K_2 are suitable constants. For an infinitesimal portion of the CNT surface:

$$di = K_1 d\sigma E_{\perp}^2 exp\left(-\frac{K_2}{E_{\perp}}\right)$$

Electron emission by CNT

Assuming ρ radius of the carbon nanotube, a cylindrical coordinate system with the axis of CNT as z-axis, and cylindrical coordinate ϑ:

$$d\sigma = \rho d\vartheta dz \qquad E_{\perp} = E\cos\vartheta$$

We can, then, write the current emitted from consider an infinitesimal portion of the CNT surface in the side-wall as:

$$di_S(E) = K_1 \rho d\vartheta dz (E\cos\vartheta)^2 exp\left(-\frac{K_2}{E\cos\vartheta}\right)$$

Electron emission by CNT

The total current emitted across the side-wall surface of the CNT is obtained by integrating on the portion of the surface facing the anode:

$$i_S(E) = K_1 \rho E^2 \int_0^L dz \int_{-\frac{\pi}{2}}^{\frac{\pi}{2}} \cos^2 \vartheta exp\left(-\frac{K_2}{E\cos\vartheta}\right) d\vartheta$$

$$= K_1 \rho E^2 L \int_{-\frac{\pi}{2}}^{\frac{\pi}{2}} \cos^2 \vartheta exp\left(-\frac{K_2}{E\cos\vartheta}\right) d\vartheta.$$

Electron emission by CNT

Recalling now that the CNT stands at an angle α with respect the line perpendicular to the electrode surface:

$$i_S(E,\alpha)=K_1\rho E^2 L\int_{-\frac{\pi}{2}}^{\frac{\pi}{2}}(\cos\vartheta\sin\alpha)^2 exp\left(-\frac{K_2}{E\cos\vartheta\sin\alpha}\right)d\vartheta$$

The current from the tip just obeys the Fowler–Nordheim equation:

$$i_T(E,\alpha) = K_1' A(E\cos\alpha)^2 exp\left(-\frac{K_2'}{E\cos\alpha}\right)$$

And the total current emitted by an oriented CNT:

$$i(E,\alpha) = i_S(E,\alpha) + i_T(E,\alpha)$$

Electron emission by CNT

C. Boero, S.Carrara / IEEE Trans. NanoBioScience (2011) 59-67

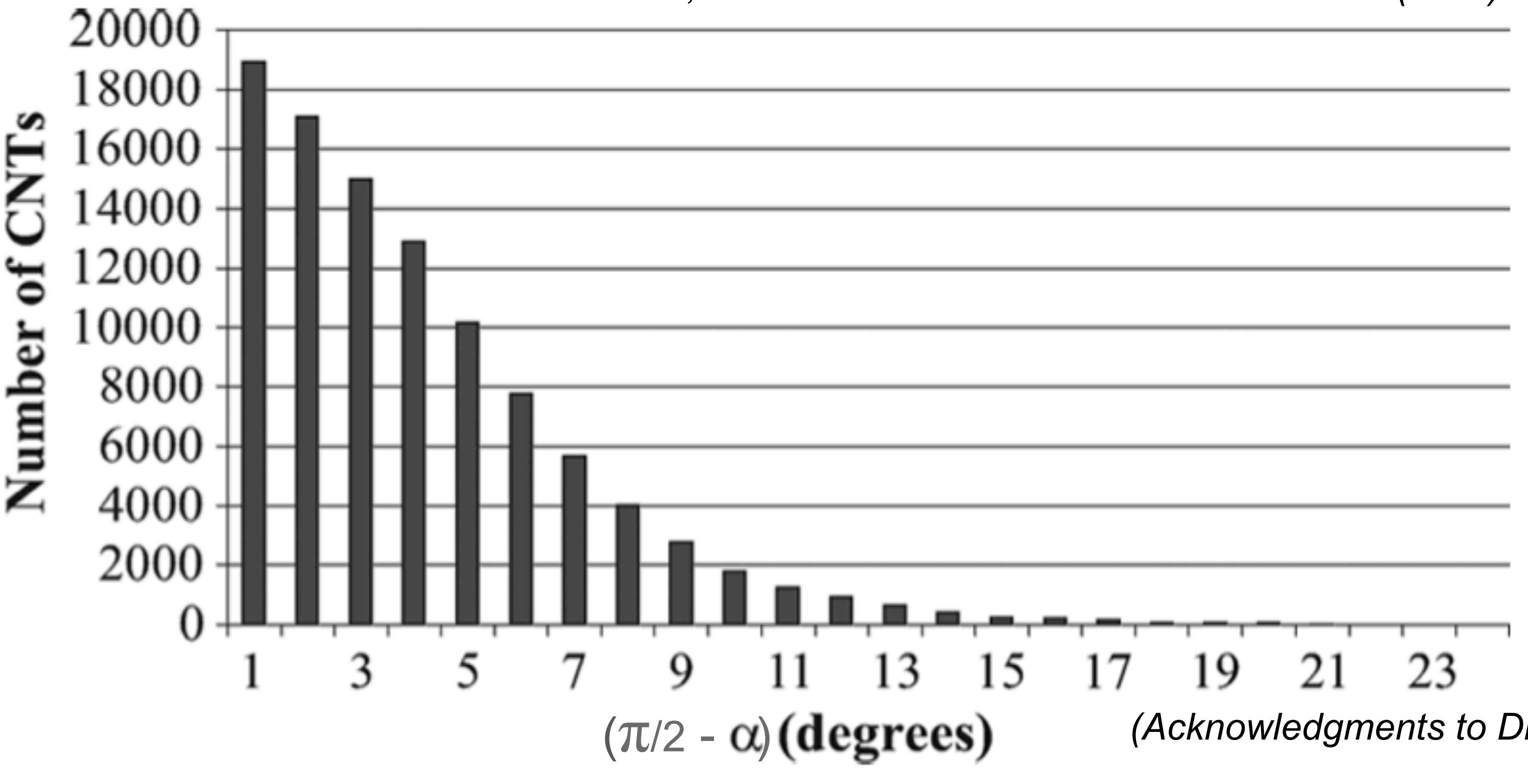

(Acknowledgments to Dino Albini)

Results from Monte Carlo simulations for the distribution of carbon nanotubes onto a flat surface

Electron emission by CNT

C. Boero, S.Carrara / IEEE Trans. NanoBioScience (2011) 59-67

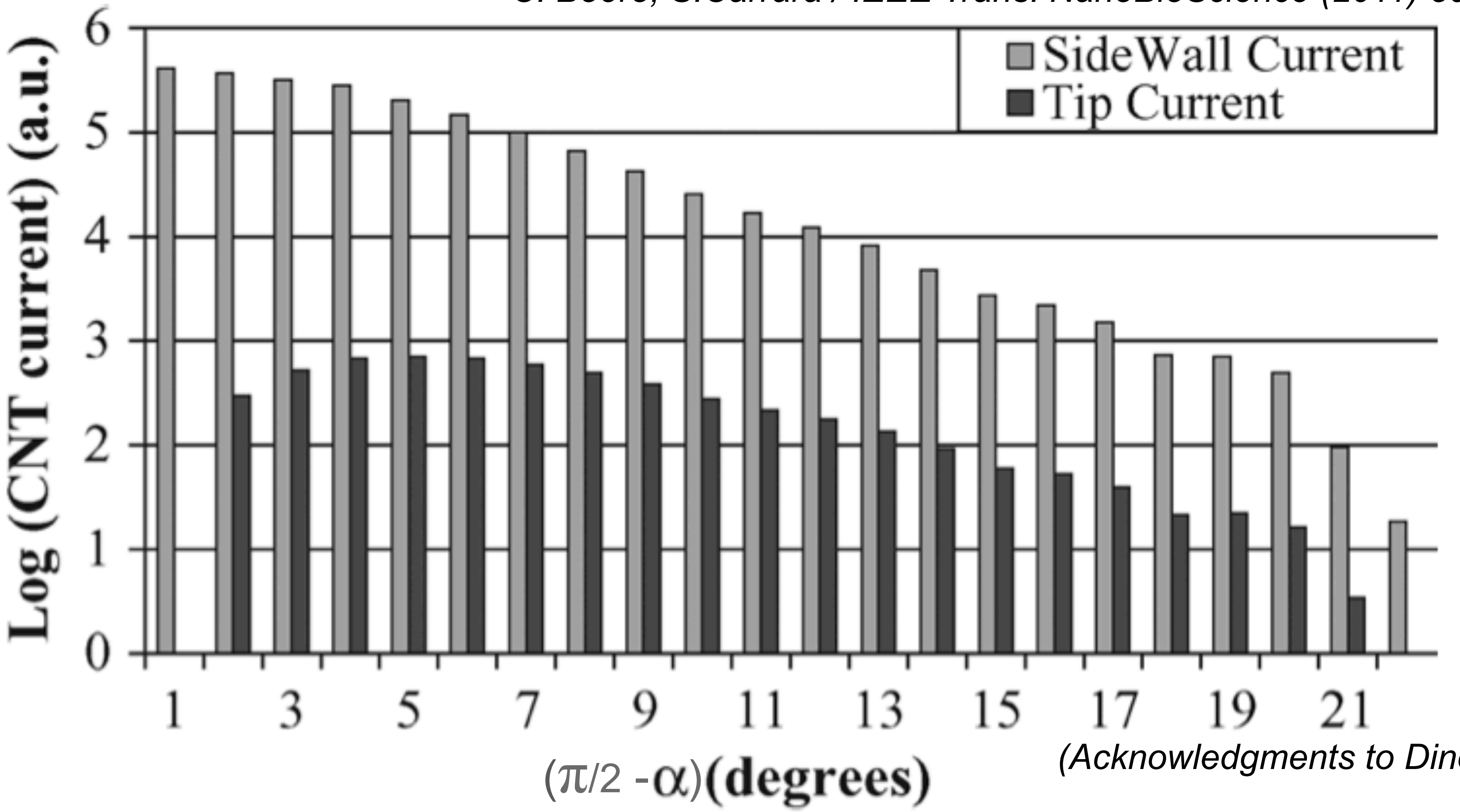

(Acknowledgments to Dino Albini)

Simulations regarding emission currents from carbon nanotubes comparing the sidewall and the tip components